Temperature effect on perfluorooctane sulfonate toxicokinetics in rainbow trout (Oncorhynchus mykiss): exploration via a physiologically based toxicokinetic model

Alice Vidal, Marc Babut, Jeanne Garric, Rémy Beaudouin

Temperature effect on perfluorooctane sulfonate toxicokinetics in rainbow trout (Oncorhynchus mykiss): exploration via a physiologically based toxicokinetic model

Alice Vidal[a], Marc Babut[a], Jeanne Garric[a], Rémy Beaudouin[b]*

[a] INRAE, RIVERLY, 5 Avenue de la Doua, CS20244, 69625 Villeurbanne Cedex, France.

[b] UMR-I 02 SEBIO, Models for Ecotoxicology and Toxicology Unit (METO), INERIS, 60550 Verneuil en Halatte, France.

*Corresponding author: remy.beaudouin@ineris.fr

Rémy Beaudouin. INERIS, Models for Ecotoxicology and Toxicology Unit (METO), Parc technologique Alata BP2, 60550 Verneuil-en-Halatte, France.

Abstract

Salmonids are poikilotherms which means that their internal temperature varies with that of water. Water temperature thus controls many of their lifecycle processes and physiological functions, which could influence the mechanisms of absorption, distribution, metabolism and excretion (ADME) of many substances, including perfluorinated alkyl substances (PFAAs). However, the processes governing the fate of PFAAs are still poorly understood in fish. Here we developed a physiologically based toxicokinetic (PBTK) model for rainbow trout (*Oncorhynchus mykiss*) to study changes in physiological functions and PFAA ADME at different temperatures. The model was calibrated using experimental data from dietary exposure to perfluorooctane sulfonate at 7°C and 19°C. Predictions of PFOS concentrations were globally satisfactory at both temperatures, when accounting for the influence of temperature on growth, ventilation rate, cardiac output, clearances, and absorption rates. Accounting for the influence of temperature on tissue–plasma partition coefficients significantly improved predicted in-organ PFOS concentrations.

Keywords: PBTK, ADME, temperature, PFOS, trout

1. Introduction

Salmonids are poikilotherms, which means their body temperature varies with that of water. Most poikilotherms are ectotherms, *i.e.* their body temperature is strictly the same as the surrounding water temperature. This makes temperature a key variable for these organisms, as it governs a number of critical processes in the fish life cycle, such as reproduction, growth and feeding rate (Grech et al. 2019; Hilton and Slinger, 1981). Rainbow trout, for example, only lay eggs once a year, when temperature and food conditions are right (Estay et al. 2012). It is well known that the amount of food consumed by fish depends directly on temperature (Wootton, 1990). A decrease in water temperature leads to a decrease in feeding level, as shown in rainbow trout where fish acclimated to colder temperature showed lower body weight gain compared to fish reared at warmer temperatures (Azevedo et al. 1998). As temperature influences feeding behaviour, it also mediates digestion efficiency. Digestive transit time decreases with increasing temperature, due to faster faecal elimination (Hofer et al. 1982, Rajasilta, 1980, Shrable et al. 1969; Fauconneau et al. 1983). Temperature also influences other physiological functions, such as cardiac output, which increases with temperature, or the relative blood flows to organs (Barron et al., 1987). Changes in blood flow also have an impact on the absorption of oxygen (and other chemicals) through gills if the relative blood flow to gills is a limiting factor (Kleinow et al., 2008). Furthermore, the dynamics of oxygen absorption through the gills is also directly affected by temperature changes, as in-water oxygen concentration decreases with increasing temperature, leading fish to accelerate their ventilation rate at higher temperatures (Kleinow et al. 2008; Fry 1971; Brett and Groves, 1979).

All these physiological modifications can affect the toxicokinetics (TK) of ingested chemicals. In fish, a decrease of temperature globally leads to a retention of organic compounds in different organs of fish (Collier et al. 1978; Paterson et al. 2007). Jimenez et al. (1987) showed in bluegill sunfish (*Lepomis macrochirus*) exposed to benzo(a)pyrene that uptake and elimination rates were lower at 13°C than at 23°C, and they went on to posit that water intake increases at warmer temperature, thereby increasing exposure. More recently, we showed that the distribution and elimination of selected perfluorinated alkyl substances (PFAAs) changed in rainbow trout exposed to the same concentration in food at different temperatures (Vidal et al., 2019a). PFAAs belong to the wider per- and polyfluorinated alkyl substances (PFAS) family, an important class of environmental contaminants with strong carbon-fluorine bonds that make them environmentally stable (Buck et al., 2011). Many PFAAs are ubiquitous in aquatic ecosystems, and some of them bioaccumulate in organisms (Houde et al., 2006; Ahrens and Bundschuh, 2014; Krafft and Riess, 2015). However, the mechanisms involved in PFAA absorption, distribution, metabolism and elimination (ADME) processes in fish are still insufficiently understood. Within the PFAA class, perfluorooctane sulfonate (PFOS), which is a strong acid, has been found in aquatic ecosystems throughout the world (Houde et al. 2006; Houde et al. 2011). Despite regulatory efforts to reduce PFOS emissions (Lindstrom et al., 2011; European Union, 2006), its environmental

concentrations are still high compared to other fluorinated compounds (Krafft and Riess, 2015; Shi et al., 2012).

We previously concluded (Vidal et al. 2019b), based on experimental data and modelling, that PFOS elimination was mainly via faeces, that elimination through gills was a relatively minor route, and that urinary elimination was negligible. We also concluded that the enterohepatic cycle is likely to play a minor role in PFOS toxicokinetics. However, these conclusions were drawn at a single exposure temperature. To push our analysis further, the next step was to study the influence of temperature on ADME processes using the same combination of experiments (Vidal et al. 2019a) and modelling. Modifications of physiological functions (fish growth, cardiac output, ventilation rate, organ perfusion) and PFOS kinetic processes (clearances, absorption rate, tissue-plasma partition coefficients) according to temperature were accounted for in the appropriate PBTK model functions. The PBTK model was developed and calibrated via a Bayesian approach using two datasets of PFOS concentrations in tissues of rainbow trout fed a PFOS-spiked diet, at 7°C and at 19°C (Vidal et al. 2019a). Finally, model predictions were evaluated using an independent dataset in which mean water temperature was 15°C (Goeritz et al. 2013).

2. Materials and methods

2.1. PBTK model accounting for the influence of water temperature

The PBTK model developed by Vidal et al. (2019b) served as the basis for this development work. Briefly, the initial model comprised ten compartments, *i.e.* arterial blood, venous blood, liver, kidney, viscera, muscle, brain, skin, gills, and carcass corresponding to the rest of the body, which thus explains residual substance concentrations in the organism (Figure A.1, in SI). For this study, we assumed that PFOS entered the organism simultaneously through diet and through the gills. Oral doses entered the gut (divided into lumen and tissue), and the compound then passed into the blood according to the absorption rate (Ku). PFOS absorption and elimination by gills was dependent on ventilation rate, which is related to oxygen consumption rate, as in Nichols et al. (1990). In the initial model, and in line with the parsimony principle, the ionizable nature of PFOS was neglected for uptake and elimination through gills, due to a lack of data to parametrize these transfers: parameters describing these processes are likely unidentifiable based on the data available (*i.e.* two or more parametrizations give equivalent predictions). Consequently, PFOS transfer through gills was modelled by simple diffusion, where 100% of PFOS present in water was absorbed. Vidal et al. (2019b) showed that this assumption efficiently models exposure to low PFOS concentrations in water. Finally, the model considered elimination by faeces, bile and urine simultaneously.

2.2. Model equations

A glossary of abbreviations, definitions, units and values for the model parameters can be found in SI, Table A.1. Parameter values are the *a posteriori* values obtained by Bayesian calibration of the PBTK model proposed by Vidal et al. (2019b) at 19°C. We thus considered 19°C as the reference temperature here. Equations used in the initial model are reported in SI, section A.1.

2.2.1. Integration of temperature effects on physiological processes

The initial model (Vidal et al. 2019b) already accounted for the temperature response of cardiac output (Qc) and the oxygen consumption rate involved in absorption and elimination by gills (VO_2), which was done using the Arrhenius function (Equation 1).

$$\boldsymbol{KT = exp\left(\left(\frac{TA}{T}\right) - \left(\frac{TA}{Texp}\right)\right)} \quad \text{(Equation 1)}$$

where *KT* is the Arrhenius correction factor, *T* is water temperature of the experiment (in Kelvin), *TA* is Arrhenius temperature, which governs the curve of the temperature-response relationship (in Kelvin), and T_{ref} is the reference temperature (in Kelvin). *KT* was then integrated into both the cardiac output (Qc, Equation 2) and oxygen consumption rate (VO_2, Equation 3) processes.

$$\boldsymbol{Qc = Qc_{ref} \times KT \times \left(\frac{BW}{BW_{Qc_{ref}}}\right)^{-0.1} \times BW} \times F_{plasma}\text{, L.h}^{-1} \quad \text{(Equation 2)}$$

where $BW_{Qc_{ref}}$ is the reference body weight (kg) at which Qc_{ref}, the reference value of the process, was recorded, *BW* is fish mass, and F_{plasma} is plasma fraction of the blood (Table A.1. in SI).

$$\boldsymbol{VO_2 = VO_{2_{ref}} \times KT \times \left(\frac{BW}{BW_{VO2_{ref}}}\right)^{-0.1} \times BW}\text{, mg}_{O2}\text{.h}^{-1} \quad \text{(Equation 3)}$$

where BW_{VO2ref} is the reference body weight (kg) at which VO_{2ref} ($mg_{O2}\,h^{-1}$), the reference value of the process, was recorded, and *BW* is body weight (kg) (Table A.1., in SI).

Barron et al. (1987) showed that the relative blood flow fraction of white muscle significantly increased according to the temperature at which rainbow trout were acclimated. This change was modelled as shown by Equation 4. As we had no information on the blood flow distribution to other organs to balance changes in muscle, we posited that the fraction of blood flow lost by each organ was proportional to their initial relative blood flow. This physiological variation was thus modelled as shown in Equations 5, 6 and 7.

$$\boldsymbol{frac_{muscle} = frac_{muscle_{ref}} \times KT} \quad \text{(Equation 4)}$$

where $frac_{muscle}$ is the relative blood flow fraction of muscle, and $frac_{muscle\_ref}$ is the reference relative blood flow fraction of muscle (Table A.1., in SI).

$$\boldsymbol{Delta_{muscle} = frac_{muscle_{ref}} \times (1 - KT)} \quad \text{(Equation 5)}$$

where $Delta_{muscle}$ is the relative change of muscle blood flow fraction according to temperature.

$$\boldsymbol{F_i = (frac_i + \frac{frac_i}{1-frac_{muscle_{ref}}} \times Delta_{muscle}) \times Q_c} \quad \text{(Equation 6)}$$

where F_i is the blood (plasma) flow of organ i and $frac_i$ is relative fraction of blood (plasma) arriving at organ i (Table A.1., in SI).

Fish growth, based on the von Bertalanffy equation (Equations 7 and 8), was controlled by the growth rate (κ, cm h^{-1}) and maximum length (Lm, cm). A further parameter (γ) takes into account the effect of food availability and temperature on growth rate, so as to minimize the number of parameters to calibrate. This parameter (γ) was calibrated on mass and length data measured at 7°C and 19°C. Indeed, for each experiment, fish were fed a temperature-dependent dose. γ was independent in each experiment, with γ = 0.55 ($IC_{95\%}$ [0.32 – 0.84]), γ = 1.51 ($IC_{95\%}$ [1.08 – 1.97]) and γ = 0.69 ($IC_{95\%}$ [0.44 – 1.01]), for the 7°C, 15°C (*i.e.* external Goeritz et al. 2013 dataset) and 19°C experiments, respectively.

$$\frac{dL}{dt} = \kappa \boldsymbol{\gamma} \times \left(1 - \frac{\boldsymbol{L}}{\boldsymbol{Lm}}\right) \quad \text{(Equation 7)}$$

$$BW = \alpha L^{\beta} \quad \text{(Equation 8)}$$

where L is the total fish length at caudal fork (cm), BW is fish body weight (kg), and α and β are allometric constants (Table A.1., in SI).

2.3.2. Integration of temperature effects on ADME processes

Equations for the absorption rate constant, for biliary, faecal and urinary clearances were corrected by the Arrhenius function as shown in Equations 9, 10, 11 and 12.

$$Ku = Ku_{ref} \times KT \quad \text{(Equation 9)}$$

where Ku is absorption rate constant (h^{-1}). Ku_{ref} is the value of the parameter in the model proposed by Vidal et al. (2019b) at 19°C taken as reference (h^{-1}). Other parameters referred to hereafter with a "ref" subscript are taken from the same source and point to parameter values at 19°C.

$$\boldsymbol{Cl_{bile} = Cl_{bile_{ref}} \times KT} \quad \text{(Equation 10)}$$

where Cl_{bile} is biliary clearance (L h^{-1}), and $Cl_{bile\ ref}$ is reference biliary clearance (L h^{-1}).

$$\boldsymbol{Cl_{faeces} = Cl_{faeces_{ref}} \times KT} \quad \text{(Equation 11)}$$

where Cl_{faeces} is faecal clearance (L h^{-1}), and $Cl_{faeces\ ref}$ is reference faecal clearance (L h^{-1}).

$$\boldsymbol{Cl_{urine} = Cl_{urine_{ref}} \times KT} \quad \text{(Equation 12)}$$

where Cl_{urine} is urinary clearance (L h^{-1}), and $Cl_{urine\ ref}$ is reference urinary clearance (L h^{-1}).

Data on the influence of temperature on tissue-blood or tissue-plasma PCs remains rare for fish, but there have been somewhat more studies in mammals (Hägerdal et al. 1975; Chen et al. 1980). Hägerdal

et al (1975) demonstrated that the brain-blood PC for xenon is directly related to temperature in rats, which can be explained by differences in the plasma solubility of the compound. We therefore integrated a temperature effect on the tissue-plasma PCs included in our model, and we tested two alternatives, *i.e.* an increase with increasing water temperature (Equation 13), or a decrease with increasing water temperature (14).

$$\boldsymbol{PC_i = PC_{i_{ref}} \times KT} \quad \text{(Equation 13)}$$

$$\boldsymbol{PC_i = PC_{muscle_{ref}} \times \frac{1}{KT}} \quad \text{(Equation 14)}$$

where PC_i is the organ-plasma partition coefficient, and PC_{i_ref} is the reference organ-plasma partition coefficient (see SI, Table A.1.).

2.3. Model calibration

The PBTK model proposed here was calibrated using data from two dietary PFOS exposure experiments in rainbow trout conducted at different temperatures, *i.e.* 7°C and 19°C (methods and results are detailed in Vidal et al. 2019a). Briefly, during 42d, adult rainbow trout were exposed to a diet spiked with a mixture of three PFAAs, including PFOS, at a nominal concentration of 500 ng g^{-1} (dry weight, dw). The exposure period was then followed by a 35d-depuration period. During both experiments, five fish were collected at 7, 14, 28, 42, 49, 56, 63 and 77 days, then sized, weighed and dissected. Blood, muscle, liver, kidney, brain, viscera, and faeces were analysed by ultra-high performance liquid chromatography-tandem mass spectrometry (UHPLC-MS/MS). PFOS concentrations in water were also measured at each sampling time, and water temperature was monitored (see SI, Section A.2.).

The calibration step only concerns supplementary parameters added here to the model already published (Vidal et al., 2019b), *i.e.* the Arrhenius temperatures (*TA*) of the different processes integrating a temperature effect. *TA* values describing cardiac output and ventilation rate, were already calibrated by Grech et al. (2019). We thus fixed our model values at 6930 K. *TA* describing other processes were calibrated by Bayesian inference. The *a priori* distributions are reported in Table 1.

For each experiment, inputs to the model were the recorded water temperature and oxygen concentration, the mean initial fish length, the food amount provided and the PFOS amount administered (based on food amount) (see SI, Section A.2.). The predicted organ concentrations were fitted to the geometric mean of observed data (n=5) for the experiments conducted by Vidal et al. (2019a). Experimental data for concentrations in organs and faeces were assumed to follow a log-normal distribution, and the error was estimated to equal 15%, corresponding to measurement errors and inter-individual variability. Error was set at 30% for viscera due to the heterogeneity of the samples (mixed stomach, intestine, spleen and pyloric caeca).

The PBTK model was calibrated using MCSim software (version 6.0.1), which is designed for Bayesian inference through the Markov Chain Monte Carlo method (Bois, 2009). Three independent

Markov chains of 10000 iterations were run for each calibration. To ensure chain convergence, we calculated the Gelman-Rubin convergence criterion (Gelman and Rubin, 1992), and analysed the correlation between all parameters and the density and distribution of prior and posterior values. The convergence diagnosis was carried out using R software (R-Core-team, 2016) in the RStudio environment (version 0.97.903).

2.4. Model evaluation

We used experimental data from Goeritz et al. (2013) to evaluate the model predictions of tissue PFOS distributions at a different temperature, as Goeritz et al. provided another dataset with mean water temperature set at 15°C. The authors reported that PFAS contamination in water analysed from the test basin was below 15 ng L^{-1} during the accumulation phase, and thus ruled out water as a significant route of uptake. As the measured concentration in water was not available, we simulated two exposure scenarios. First, exposure to PFOS was only modelled by diet (172.0 ±13 µg kg^{-1} dw), with PFOS concentration in water set to 0 ng L^{-1}. Second, in addition to being exposed by diet, fish were assumed to uptake PFOS from water through the gills, with PFOS concentration set to the upper limit concentration reported in Goeritz et al. (2013), *i.e.* 15 ng L^{-1}. Predictions of PFOS concentrations based on these two exposure scenarios were compared to the observed concentrations in all organs.

2.5. Relative importance of the temperature effect on the different ADME processes

To identify the processes affecting TK variations that are due to temperature and responsible for the PFOS TK changes, we proceeded by backward selection of the variables, removing variables stepwise from the model: starting from the model in which temperature was integrated in all processes, the variable with the lowest weight was removed from the model and BIC (Bayesian Information Criterion) values were compared with and without this variable. As the number of calibrated parameters depends on the processes integrated into the model, we compared the accuracy of the different models using the BIC to weight the quality of model fit with the model complexity (Spiegelhalter *et al.* 2014). To assess the quality of prediction, we calculated the ratio of each BIC for the different simplified versions of the model to the BIC of the reference model (temperature correction integrated on physiological parameters and substance-specific parameters).

To study the effect of the temperature on the fate of PFOS through the organism, we also explored variations in physiological functions and variations in kinetic processes at different theoretical temperatures chosen according to Raleigh et al. (1984), *i.e.* 4, 8, 12 16 and 20°C. For each temperature, the dissolved oxygen concentration was calculated according to the empirical relationship provided by Truesdale et al. (1955), *i.e.* 12.7, 11.2, 9.4, 7.2, 4.2 mg L^{-1}, respectively. The parameter (γ), which accounts for the effect of temperature on growth rate, was linearly interpolated from the values adjusted at 7°C and 19°C, *i.e.* 0.51, 0.56, 0.61, 0.66, 0.71, respectively. The food and water exposure scenarios were those of the experiment conducted at 19°C.

3. Results

3.1. Modelled impact of temperature on physiological processes

Fish growth was successfully calibrated, and thus provided simulations in good agreement with observed data, for both temperatures (Figure 1). Growth rate did not monotonously increase with temperature, as the daily feeding rates were different between the different experiments (0.5%, 2.6%, and 1.0% of fish average live weight for experiments at 7 °C, 15°C and 19 °C, respectively).

To assess the integration of temperature into physiological processes, the value of the parameter TA fitted for cardiac output was generalised to all the physiological processes and the predictions were compared against observed data referenced in the literature (Barron et al. 1987; Myrick and Cech, 2000; Elliott, 1969; Figure 2). Arrhenius law allowed to acceptably explain changes in the ventilation rate (Figure 2.A). The model fitted the Elliott (1969) data well, but it was not in good agreement with the data from Myrick and Cech (2000) who surprisingly reported that ventilation rate was practically independent of water temperature. Arrhenius law also allowed to correctly explain cardiac output (Figure 2.B) and muscle perfusion (Figure 2.C), as the predictions were in good agreement with experimental data.

3.2. Calibration results: *a posteriori* distributions of Arrhenius temperatures

The chains converged successfully for all calibrated parameters, *i.e.* Arrhenius temperatures for each kinetic process, with posterior distributions that were narrower compared to prior distributions (see SI, Figure A.5a). The Gelman and Rubin criterion was always between 0.9 and 1.03 for all parameters (data not shown). Means (± standard deviation) and 95% credibility intervals (95% CI) of the *a posteriori* distributions are given in Table 1.

Simulated PFOS concentrations given by the model are presented in Figure 3. The daily measured temperatures and mean oxygen concentration were used as input to predict the concentrations at 7°C and explained the concentration fluctuation. Conversely, at 19°C, the model used mean measured temperature and oxygen concentration (both parameters were nearly constant). As expected, at our reference temperature 19°C, model predictions showed good fit with experimental data. At 7°C, the model gave substantially better predictions of PFOS concentrations in blood, liver and muscle when temperature effects on ADME processes were integrated (see SI, Figure A.4 and A. 6). However, the model still underestimated muscle concentration at the end of the exposure and it slightly underestimated blood concentration during the exposure period but overestimated blood concentration during the depuration phase. This pattern in the blood could explain the kidney and viscera profiles in which PFOS concentration was also slightly underestimated during the exposure period. PFOS concentrations in faeces were not well predicted and were clearly under-estimated for the depuration phase. Nevertheless,

as all predicted concentrations other than faeces were globally within a range of two times the actual concentrations, the model predictions showed good fit with experimental data.

3.3. Model evaluation

To evaluate the capacity of the PBTK model to predict PFOS concentrations to at temperatures other than 7°C and 19°C, a PFOS exposure scenario was purpose-devised based on the experimental design given by Goeritz et al. (2013). Figure 4 reports the predictions given by the current PBTK model. In cases where PFOS absorption was exclusively by diet, the model accurately predicted the experimental data (Figure 4). Indeed, most predictions were within a range of two times the measured concentrations (SI, Figure A.7). However, in the case where we considered PFOS absorption by gills using the worst-case scenario (constant exposure to the maximal value reported), all predictions were over-estimated (Figure 4) by over two times the measured concentrations (SI, Figure A.7).

3.4. Relative importance of the temperature effect on the different ADME processes

Table 2 reports the BIC values of simplified versions of the model provided by backward selection of the variables. Results showed that the best model was the most complex model integrating temperature effects on all physiological and kinetic processes. Table 2 also shows that integrating the temperature effect on partition coefficients significantly improved the model.

We also explored the effects of temperature on fate of PFOS in the organism for physiological functions (Figure 5) and for kinetic processes (Figure 6). In Figure 5, as expected, values of physiological processes steadily increased over time due to fish growth (Equations 2 and 3). Higher temperatures led to faster cardiac output, ventilation rate and-blood flow to muscle (Figure 5.A, 5.B and 5.F). Conversely, blood flow to other organs decreased at 20°C (Figure 5.C, 5.D and 5.E).

In the exposure scenario used in this section, rainbow trout were exposed to PFOS via diet for 42d, while exposure via water was held constant through the whole period (0.8 ng L^{-1}). The relative amounts of PFOS excreted via the different pathways were calculated as the ratio between quantity of PFOS excreted by each route and quantity of PFOS administered via diet and water. The quantity of PFOS excreted via urine, bile and faeces increased with temperature (Figure 6.A and 6.C). The difference between the amount absorbed via diet and water and the fraction excreted by bile and faeces represents the unabsorbed fraction of PFOS (Figure 6.E and 6.F). Gill excretion showed a non-monotonic profile with a minimal contribution to overall excretion at 8°C (Figure 6.B). Moreover, the efficiency of PFOS assimilation (Figure 6.E) varies mainly according to PFOS fraction absorbed from food (assimilation from water is 100% efficient). The relative contribution of food to PFOS absorption thus decreases with temperature (Figure 6.F). PFOS assimilation showed small variations and was also non-monotonic with a minimal value at 12°C. Finally, the relative weight of food and water in PFOS absorption was clearly affected by temperature: at low temperature, nearly all absorption was due to food contamination, whereas the relative contribution of water increased to more than 30% at 20°C.

4. Discussion

The model presented here accurately fits the PFOS concentration kinetics recorded in organs at two different temperatures by Vidal et al. (2019a), meaning that the PBTK model calibration step was successful. Furthermore, the current model also showed accurate prediction on the independent dataset obtained from Goeritz et al. (2013), even in gills and skin which are tissues for which partition coefficients have not yet been calibrated. Moreover, even though the nominal PFOS concentration in food was the same as in the experiments by Vidal et al. (2019a), the amounts of food were adjusted according to fish weight and temperature, and these changes were successfully accounted for in the simulations. These results suggest that the model can be used to describe PFOS fate in fish, under different water temperatures and conditions, and to confidently describe temperature effects on each ADME process. The lowest BIC (Table 2) was provided by the model in which temperature was integrated in all physiological and kinetic processes. This was supported by the results of *a posteriori* distribution calibration, showing similar Arrhenius temperature values for all processes (Table 1), which means that all processes co-participated in the variation of PFOS TK. The BIC ratios also demonstrated that integrating temperature in the tissue-plasma partition coefficients affected PFOS TK (Table 2) more than other TK processes.

To our knowledge, the temperature effect on blood-organ PCs has never been studied in teleost fish. In mammals, Hägerdal et al (1975) demonstrated that the brain-blood PC for xenon is directly related to temperature in rats, which can be explained by differences in the plasma solubility of the compound. Fisher et al. (2018) integrated the effect of temperature on the air-water PCs of chemical substances using equations similar to the Arrhenius function. Our results also clearly show that temperature effects on PCs played an important role in PFOS bioaccumulation in liver and in muscle. Here, the Arrhenius law was integrated in the PC between liver and plasma, whereas the inversed Arrhenius law was used to characterize the change in PC between muscle and plasma. This empirical modelling approach substantially improved predictions of PFOS concentrations in muscle in the 7°C experiment. Observations in mammals suggest that plasma solubility (bound to serum albumin or to fatty-acid-binding proteins) could be responsible for the variation of PCs with temperature (Salvalaglio et al. 2010; Luo et al. 2012). In addition, interactions with the phospholipid bilayer (Nouhi et al. 2018), *i.e.* temperature effect on membrane fluidity, could also be partially responsible for these phenomena. These processes are likely the same in poikilotherm species. However, further work is needed to confirm these assumptions and to understand the inverse variation of PCs between the different tissues. This correction of the PC balanced out the effect of temperature on accelerated muscle blood flow at 19°C, which means that higher temperatures promote bioaccumulation in this tissue. However, PFOS concentrations in muscle were still under-estimated at 7°C.

In other organs, predicted PFOS concentrations at both temperatures showed good fit with observed data (Vidal et al. 2019a), except in the brain. The model overestimated PFOS concentrations at 7°C, suggesting that simulated PFOS absorption was too fast. In humans, the blood-brain barrier is relatively non-permeable to ions and polar molecules (Macdonald et al., 2010; Ge et al., 2005). The blood–brain barrier was not modelled here, and it might have limited PFOS penetration into the brain. A recent study of the accumulation of different chain-length PFAAs (and some of their polyfluorinated precursors) in *Globicephala melas* (Dassuncao et al. 2019) suggested that compounds with <10 perfluorinated carbons (thus including PFOS) are unbale to efficiently cross the blood−brain barrier, and that compound > 10 perfluorinated carbons accumulate in the brain. Their results were consistent with elevated levels of long-chain PFAAs that have been observed in the brain of other mammals (Greaves et al. 2012; Ahrens et al. 2009), whereas the only shorter chain compounds detected (< 7 perfluorinated carbons) was perfluorohexane sulfonate (Ahrens et al. 2009). Therefore, predictions of PFOS concentrations at 7°C might be improved by accounting for affinity to phospholipids, which are involved in PFOS blood-brain barrier crossing.

Accordingly, to gain further insight into the mechanisms involved in PFOS bioaccumulation in fish, it would be usefully informative to consider binding between PFAAs and proteins of interest, such as fatty-acid-binding proteins and albumin (Ng and Hungerbühler, 2013; Zhong et al. 2019; Martin et al. 2003; Consoer et al. 2016; Jones et al. 2003; Manera et al. 2006). Indeed, protein-chemical binding affinities are temperature-sensitive, since the equilibrium association constant is directly dependent on this parameter (Ng and Hungerbühler, 2015). Note too that we did not integrate into the model the ionizable nature of PFOS for uptake and elimination through gills, whereas water temperature might affect ionization equilibrium and, in turn, impact the absorption efficiency of PFOS in water. However, we were unable to find any literature to support this hypothesis.

It has been demonstrated that a temperature decrease enhances the accumulation of organic compounds both in whole fish (Paterson et al. 2007) and in specific fish organs (brain, liver, kidney and blood; Collier et al. 1978). This indicates that the elimination rate changed directly with temperature. Several studies supported this hypothesis: for example, Haywood and Clapp (1942) showed that urinary flow in *Catostomus commersonii* is lower in winter compared to spring, and this same observation has also been reported for some cyprinid fish, such as *Carassius auratus* L (Mackay, 1974). The PFOS kinetics found here (Figure 3 and 6) converge with this hypothesis, despite the fact that urine is a secondary excretion pathway for PFOS (Vidal et al, 2019b). Other studies have demonstrated an increase of biliary excretion with temperature in rainbow trout (Curtis, 1983; Curtis et al. 1986; Kemp et Curtis, 1987), which was thought to be linked to the modification of blood flow to liver, as it controls biliary excretion (Kleinow et al. 2008). A temperature change might also influence gut transit rate in fish. When acclimation temperature increased, gastro-intestinal transit time became shorter and faecal elimination became faster (Hofer et al. 1982; Rajasilta, 1980; Shrable et al. 1969; Fauconneau et al. 1983).

Our model showed fairly correct predictions of the daily fluctuations of PFOS concentration in faeces (*i.e.* the fraction eliminated by bile and the non-absorbed fraction) during the exposure phase, as the observed data were within the range of predicted min–max values for the daily fluctuations (caused by the daily feeding intake). However, during the depuration phase, PFOS concentration in faeces was underestimated at 7°C when faecal concentration only represented bile excretion. As our model integrated a decreasing effect of the temperature on gut transit rate and bile excretion, these results are unexpected (about 30% of the maximal rate at 7°C; see SI, Figure A.5b). One explanation might be that the Arrhenius law and/or this parameterization do not sufficiently capture the temperature-induced variation in gut transit rate and bile excretion.

Concerning the dynamics of absorption and excretion by gills, it is well known that oxygen absorption is temperature-sensitive. This is explained by the fact that oxygen concentration in water decreases with temperature, thus forcing the fish to accelerate its ventilation rate (Kleinow et al. 2008; Fry 1971; Brett et Groves, 1979). This increased water flow may promote exposure to waterborne contaminants at higher temperatures (Jimenez et al. 1987). In addition, temperature might alter the molecular structure of the branchial epithelium, modifying its permeability to compounds (Crockett and Hazel, 1995). Some recent PBTK models have described the effect of temperature on ventilation in fish (Péry et al. 2014; Brinkmann et al. 2014; Brinkmann et al. 2015; Grech et al. 2019). Results of the PBTK model developed by Vidal et al. (2019b) showed the importance of the branchial pathway to plot PFOS TK. Here, we integrated temperature effects on the ventilation process and on the blood-water PC. This modelling showed that elimination through gills had a non-monotonic profile, with a minimum at 8°C. This non-monotonic profile probably results from the combination of decreased oxygen concentration in water, increased cardiac output and increased ventilation rate with the increase in water temperature (Figure 6). In addition, the fraction of PFOS absorbed from water clearly increased with temperature to about 30% at 20°C. In the current model, we modelled absorption and elimination through gills as simply as possible, by considering that all PFOS present in water could enter through the gills. Since PFOS is a strong acid, present at > 99.99% in its ionic form at gills, Erickson et al. (2006) integrated in their model three additional processes purpose-developed for absorption and elimination of ionizable compounds. However, new experimental data have to be produced before we can integrate these processes and the effects of temperature on them in order to quantify their relative weight on the certainty of predicted PFOS concentrations in fish.

Global warming and associated shifts in the distribution of ectothermic organisms has prompted a surge in research into the physiological mechanisms governing cold and heat tolerance. Salmonids are ectotherms, and so water temperature controls many of their lifecycle processes, including growth (Azevedo et al. 1998; Hilton et Slinger, 1981), cardiac output (Barron et al. 1987), ventilation rate (Elliott, 1969, Myrick and Cech, 2000), and more. To be closer to physiological reality, which is important in risk assessment, Vidal et al. (2019b) integrated the effect of temperature in their PBTK

model developed to describe PFOS fate. In fish, PFOS and temperature are both known to influence spontaneous swimming behaviour, social interactions, routine metabolic rate, net energy cost of transport, and critical swimming speed for example (Xia et al., 2015). Here, we first integrated the effect of temperature on fish growth to explain the dilution of PFOS concentration, and then like Grech et al. (2019), we used the Arrhenius law to describe the influence of temperature on other processes. To date, few published models have factored this environmental variable to explain the TK of compounds. Our findings showed that accounting for the effect of temperature on both physiological functions and ADME processes significantly improves mechanistic TK modelling. Moreover, prompted by ongoing climate change, a number of scientists have turned to investigate temperature effects on the bioaccumulation of xenobiotics (Xu et al., 2010; Houde et al., 2011). In fish, it has been shown that water temperature can influence the bioaccumulation of organic compounds (Paterson et al. 2007; Jimenez et al. 1987), especially PFAAs (Vidal et al. 2019a). Vidal et al. (2019a) demonstrated that a change in temperature led to a change in PFAA distribution in adult rainbow trout. These observations are further supported by the results obtained in the present study, which provides new insights on the influence of temperature, suggesting that temperature is an important factor for explaining variations in PFOS kinetic processes. Moreover, the current PBTK model, based on the digressive approach, was able to identify processes sensitive to temperature changes, which might explain the variations in PFOS TK.

5. Conclusion

The findings of this study argue that our model makes a useful tool for risk assessment. Only a few PBTK models are applicable to PFAAs, whereas these chemicals are still in widespread production. Several exposure scenarios spanning a wide range of water-stream temperatures can now be tested thanks to this PBTK model, which simultaneously considers several absorption and excretion pathways. This PBTK model makes a relevant and timely update of the model developed by Vidal et al (2019b), since it accounts for an influential variable for compound bioaccumulation in fish.

Acknowledgements

The experiments were funded by the Rhone-Mediterranean and Corsica Water Agency. Alice Vidal received doctoral fellowship grant support (ARC3 Environnement) from the Rhone-Alps Region. We thank Charline Gesset, Patrick Chevre and Louis Jacob (Irstea, St-Seurin-sur-l'Isle experimental station) for their kind and active support during the experiments, and Ina Goeritz and Christian Schlechtriem (Fraunhofer Institute for Molecular Biology and Applied Ecology, Schmallenberg, Germany) for providing data for the 15°C experiment. We also thank Glen McCulley (Metaform Langues, Clermont-

Ferrand, France) for copy-editing the manuscript. The authors also thank the three anonymous reviewers for their helpful suggestions for improvement and their constructive remarks.

References

Ahrens L. and Bundschuh M. 2014. Fate and effects of poly- and perfluoroalkyl substances in the aquatic environment: A review. Environmental Toxicology and Chemistry 33: 1921–1929.

Ahrens L., Siebert U., Ebinghaus R. 2009. Total body burden and tissue distribution of polyfluorinated compounds in harbor seals (Phoca vitulina) from the German Bight. Marine Pollution Bulletin 58: 520−525.

Azevedo P.A., Cho C.Y., Leeson S., Bureau D.P. 1998. Effects of feeding level and water temperature on growth, nutrient and energy utilization and waste outputs of rainbow trout (*Oncorhynchus mykiss*). Aquatic Living Resources 11: 227–238.

Barron M.G., Tarr B.D., Hayton W.L. 1987. Temperature-dependence of cardiac output and regional blood flow in rainbow trout, *Salmo gairdneri Richardson*. Journal of Fish Biology 31:735–744.

Bois F.Y. 2009. GNU MCSim. Journal Bioinformatics, 25: 1453–1454

Brett J.R. and Grove T.D.D. 1979. Physiological energetic. In: Hoar WS, Randall DJ, Brett JR (Eds.), Fish Physiology. Bioenergetics and Growth, vol. VIII. Academic Press, New York, 279 – 352.

Brinkmann M., Eichbaum K., Kammann U., Hudjetz S., Cofalla C., Buchinger S., Reifferscheid G., Schüttrumpf H., Preuss T., Hollert H. 2014. Physiologically-based toxicokinetic models help identifying the key factors affecting contaminant uptake during flood events. Aquatic Toxicology, 152, 38–46.

Brinkmann M., Freese M., Pohlmann J.D., Kammann U., Preuss T. G., Buchinger S., Reifferscheid G., Beiermeister A., Hanel R., Hollert H. 2015. A physiologically based toxicokinetic (PBTK) model for moderately hydrophobic organic chemicals in the European eel (*Anguilla anguilla*). Science of the Total Environment. 536,279-287.

Buck R.C., Franklin J., Berger U., Conder J.M., Cousins I.T., de Voogt P., Jensen A.A., Kannan K., Mabury S.A., van Leeuwen S.P.J., 2011. Perfluoroalkyl and polyfluoralkyl substances in the environment: terminology, classification, and origins. Integrated Environmental Assessment and Management 7: 513-541.

Cameron J. N and Davis J.C. 1970. Gas exchange in rainbow trout (Salmo gairdneri) with varying blood oxygen capacity. Journal of the Fisheries Research Board of Canada. 27: 1069-1085.

Chen R., Fan F.C., Kim S., Jan K.M., Usami S., Chien S. 1980. Tissue-blood temperature partition coefficient for xenon: and hematocrit dependence. Journal of Applied Physiology 49: 178–183.

Collier T.K., Thomas L.C., Malins D.C. 1978. Influence of environmental temperature on disposition of dietary naphthalene in coho salmon (*Oncorhynchus kisutch*): isolation and identification of individual metabolites. Comparative Biochemistry and Physiology Part C: Comparative Pharmacology 61, 23–28.

Consoer D.M., Hoffman A.D., Fitzsimmons P.N., Kosian P.A., Nichols J.W. 2016. Toxicokinetics of Perfluorooctane Sulfonate in Rainbow Trout (*Oncorhynchus Mykiss*). Environmental Toxicology and Chemistry 35: 717–727.

Crockett E. and Hazel J. 1995. Cholesterol levels explain inverse compensation of membrane order in brush border but not homeoviscous adaptation in basolateral membranes from the intestinal epithelia of rainbow trout. Journal of Experimental Biology 198: 1105-13.

Curtis L.R. 1983. Glucuronidation and biliary excretion of phenolphthalein in temperature acclimated steelhead trout (*Salmo gairdneri*). Comparative Biochemistry and Physiology Part C: Comparative Pharmacology. 76, 107-111.

Curtis L.R., Kemp C.J., Svec A.V. 1986. Biliary excretion of [14C]taurocholate by rainbow trout (*Salmo gairdneri*) is stimulated at warmer acclimation temperature. Comparative Biochemistry and Physiology Part C: Comparative Pharmacology. 84, 87-90.

Dassuncao C., Pickard H., Pfohl M., Tokranov A.K., Li M., Mikkelsen B., Slitt A., Sunderland E.M. 2019. Phospholipid levels predict the tissue distribution of poly- and perfluoroalkyl substances in a marine mammal. Environmental Science and Technology Letter 6: 119-125.

Davis J.C. and Cameron J. N. 1971. Water flow and gas exchange at the gills of rainbow trout, *Salmo gairdneri.* Journal of Experimental Biology. 54: 1-18.

Elliott J.W. 1969. The oxygen requirements of chinook salmon. The Progressive Fish-Culturist 31: 67-73.

Erickson R.J., Mckim J.M., Lien G.J., Hoffman A.D., Batterman L.S. 2006. Uptake and elimination of ionizable organic chemicals at fish gills: i. Model formulation, parameterization, and behavior. Environmental Toxicology and Chemistry, 25, 1512–1521.

Estay F., Colihueque N., Araneda C. 2012. Comparison of Oogenesis and Sex Steroid Profiles between Twice and Once Annually Spawning of Rainbow Trout Females (*Oncorhynchus mykiss*). Scientific World Journal 2012: 986590.

European Union. 2006. Directive 2006/122/EC of the European Parliament and of the Council of 12 December 2006 amending for the 30th time Council Directive 76/769/EEC on the approximation of the laws, regulations and administrative provisions of the Member States relating to restrictions on marketing and use of certain dangerous substances and preparations (perfluorooctane sulfonates). Official Journal of the European Union L372:32–34.

Fauconneau B., Choubert G., Blanc D., Breque J. Luquet P. 1983. Influence of environmental temperature on flow rate of foodstuffs through the gastrointestinal tract of rainbow trout. Aquaculture 34 : 27-39.

Fisher C., Siméon S., Jamei M., Gardner I., Bois F.Y. 2018. VIVD: Virtual in vitro distribution model for the mechanistic prediction of intracellular concentrations of chemicals in in vitro toxicity assays. Toxicology in Vitro 58: 42–50.

Fry F.E.J. 1971. The effects of environmental factors on the physiology of fishes. In Fish Physiology (Edited by Hoar W. S. and Randall D. J.). Academic Press. New York 6: 1-98.

Ge S.J., Song L., Pachter J.S. 2005. Where is the blood-brain barrier... really? Journal of Neuroscience Research 79: 421-427.

Gelman A. and Rubin D. 1992. Inference from iterative simulation using multiple sequences. Statistical science 7: 457–511.

Goeritz I., Falk S., Stahl T., Schäfers C., Schlechtriem C. 2013. Biomagnification and tissue distribution of perfluoroalkyl substances (PFASs) in market-size rainbow trout (*Oncorhynchus mykiss*). Environmental Toxicology and Chemistry 32: 2078–2088.

Greaves A.K., Letcher R.J., Sonne C., Dietz R., Born E.W. 2012. Tissue-specific concentrations and patterns of perfluoroalkyl carboxylates and sulfonates in East Greenland polar bears. Environmental Science and Technology 46: 11575−11583.

Grech A., Tebby C., Brochot C., Bois F., Bado-Nilles A., Dorne J.L., Quignot N., Beaudouin R. 2019. Generic physiologically-based toxicokinetic modelling for fish: integration of environmental factors and species variability. Science of the Total Environment 651: 516-531.

Hägerdal M., Harp J., Nilsson L., Siesjöu B.K. 1975. The effect of induced hypothermia upon oxygen consumption in the rat brain. Journal of Neurochemistry 24: 311–316.

Haywood C. Clapp M.J. 1942. A note on the freezing-points of the urines of two fresh- water fishes: the catfish (*Ameiurus nebulosus*) and the sucker (*Catostomus commersonff*). Biology Bulletin 83: 363-366.

Hilton J.W., Slinger S.J. 1981. Nutrition and feeding of rainbow trout. Canadian Special Publication of Fisheries and Aquatic Sciences, 55: 14.

Hofer R., Forstner H. Rettenwander R., 1982. Duration of gut passage and its dependence on temperature and food consumption in roach, *Rutilus rutilus L*: laboratory and field experiments. Journal of Fish Biology 20: 289-299.

Houde M., De Silva A.O., Muir D.C.G., Letcher R.J. 2011. Monitoring of perfluorinated compounds in aquatic biota: an updated review. Environmental Science and Technology 45: 7962–7973.

Houde M., Martin J.W., Letcher R.J., Solomon K.R., Muir D.C. 2006. Biological monitoring of polyfluoroalkyl substances: a review. Environmental Science and Technology 40 : 3463–3473.

Jimenez B.D., Cirmo C.P., McCarthy J.F. 1987. Effects of feeding and temperature on uptake, elimination and metabolism of benzo(a) pyrene in the bluegill sunfish (*Lepomis macrochirus*). Aquatic Toxicology 10:41–57.

Jones P.D., Hu W., De Coen W., Nested J.L., Giesy J.P. 2003. Binding of perfluorinated fatty acids to serum proteins. Environmental Toxicology and Chemistry 22: 2639–2649.

Kemp C.J. and Curtis L.R. 1987. Thermally Modulated Biliary Excretion of [14C]Taurocholate in Rainbow Trout (*Salmo gairdneri*) and the Na+,K+-ATPase. Canadian Journal of Fisheries and Aquatic Sciences 44: 846-851.

Kiceniuck J. W. and Jones D. R. 1977. The oxygen transport system in trout (*Salmo gairdneri*) during sustained exercise. Journal of Experimental Biology. 69: 247-260.

Kleinow K.M. Nichols J.W., Hayton W.L., McKim J.M., Barron M.G., 2008. Toxicokinetics in fishes. In: Hinton D., Di Giulio R (eds). The Toxicology of Fishes. CRC Press, Boca Raton, p 55-152.

Krafft M.P., Riess J.G. 2015. Per- and polyfluorinated substances (PFASs): Environmental challenges. Current Opinion in Colloid and Interface Science 20: 192–212.

Lindstrom A.B., Strynar M.J., Libelo E.L., 2011. Polyfluorinated Compounds: Past, Present, and Future. Environmental Science and Technology 45: 7954-7961.

Luo Z., Shi X., Hu Q., Zhao B., Huang M. 2012. Structural evidence of perfluorooctane sulfonate transport by human serum albumin. Chemical Research in Toxicology 25: 990-992

Macdonald J.A., Murugesan N., Pachter J.S. 2010. Endothelial Cell Heterogeneity of Blood-Brain Barrier Gene Expression Along the Cerebral Microvasculature. Journal of Neuroscience Research 88: 1457-1474.

Mackay W.C. 1974. Effect of Temperature on Osmotic and Ionic Regulation in Goldfish, *Carassius auratus L*. Journal of comparative physiology A 88: 1–19.

Manera M., Britti D. 2006. Assessment of blood chemistry normal ranges in rainbow trout. Journal of Fish Biology 69: 1427−1434.

Martin J.W., Mabury S.A., Solomon K.R., Muir D.C.G. 2003. Dietary accumulation of perfluorinated acids in juvenile rainbow trout (*Oncorhynchus mykiss*). Environmental Toxicology and Chemistry 22: 189-195.

Myrick C.A. and Cech J.J. 2000. Temperature influences on California rainbow trout physiological performance. Fish Physiology and Biochemistry 22: 245-254.

Neumann P., Holeton G. F. Heisler N. 1983. Cardiac output and regional blood flow in gills and muscles after exhaustive exercise in rainbow trout (*Salmo gairdnero*). Journal of Experimental Biology. 105: 1-14.

Ng C.A. and Hungerbuehler K. 2013. Bioconcentration of Perfluorinated Alkyl Acids: How Important Is Specific Binding? Environmental Science and Technology 47: 7214–7223.

Ng C.A. and Hungerbuehler K. 2015. Exploring the Use of Molecular Docking to Identify Bioaccumulative Perfluorinated Alkyl Acids (PFAAs). Environmental Science and Technology 49: 12306−12314.

Nichols J.W., McKim J.M., Andersen M.E., Gargas M.L., Clewell H.J., Erickson R.J. 1990. A physiologically based toxicokinetic model for the uptake and disposition of waterborne organic chemicals in fish. Toxicology and Applied Pharmacology. 106: 433-447.

Nouhi S., Ahrens L., Campos Pereira H., Hughes A.V., Campana M., Gutfreund P., Palsson G.K., Vorobiev A., Hellsing M.S. 2018. Interactions of perfluoroalkyl substances with a phospholipid bilayer studied by neutron reflectometry. Journal of Colloid and Interface Science 511: 474-481.

Paterson G., Drouillard K.G., Haffner G.D. 2007. PCB elimination by yellow perch (Perca flavescens) during an annual temperature cycle. Environmental Science and Technology 41: 824–829.

Péry A.R.R., Devillers J., Brochot C., Mombelli E., Palluel O., Piccini B., Brion F., Beaudouin R. 2014. A Physiologically Based Toxicokinetic Model for the Zebrafish Danio rerio. Environmental Science and Technology. 48: 781-790.

R Core Team (2016) R: A Language and Environment for Statistical Computing. R Foundation for Statistical Computing, Vienna, Austria.

Rajasilta M. 1980. Food consumption of the three-spined stickleback (Gasterosteus aculeatus L.). Annales Zoologici Fennici. 17, 123-126.

Raleigh R.F., Hickman T., Solomon R. C. et Nelson P. C. 1984 Habitat Suitability Index Models: Rainbow trout. U. S. Fish Wildlife Service Report. FWS/OBS-82/10.60

Salvalaglio M., Muscionico I., Cavallotti C. 2010. Determination of energies and sites of binding of PFOA and PFOS to human serum albumin. Journal of Physical Chemistry B 114: 14860-14874.

Shi Y., Wang J., Pan Y., Cai Y. 2012. Tissue distribution of perfluorinated compounds in farmed freshwater fish and human exposure by consumption. Environmental Toxicology and Chemistry 31: 717–723.

Shrable J.B., Tiemeier O.W. Deyoe C.W. 1969. Effects of Temperature on Rate of Digestion by Channel Catfish. The Progressive Fish-Culturist. 31: 131-138.

Spiegelhalter D.J., Best N.G., Carlin B.P. Van der Linde A. 2014. The deviance information criterion: 12 years on. Journal of the Royal Statistical Society 76: 485–493.

Vidal A., Babut M., Garric J., Beaudouin R. 2019b. Elucidating the fate of perfluorooctanoate sulfonate using a rainbow trout (*Oncorhynchus mykiss*) physiologically-based toxicokinetic model. Science of the Total Environment 691: 1297–1309.

Vidal A., Lafay F., Daniele G., Vulliet E., Rochard E., Garric J., Babut, M. 2019a. Does water temperature influence the distribution and elimination of perfluorinated substances in rainbow trout (*Oncorhynchus mykiss*). Environmental Science and Pollution Research 26: 16355–16365.

Wood C. M. and Shelton G. 1980. Cardiovascular dynamics and adrenergic responses of rainbow trout in vivo. Journal of Experimental Biology. 87: 247-270.

Wootton R. J. 1990. Feeding Ecology of Teleost Fishes. Springer Netherlands, Dordrecht, p 32-72

Xia J.G., Nie L.J., Mi X.M., Wang W.Z., Ma Y.J., Cao Z.D., Fu S.J. 2015. Behavior, metabolism and swimming physiology in juvenile *Spinibarbus sinensis* exposed to PFOS under different temperatures. Fish Physiology and Biochemistry 41: 1293–1304.

Xu C., Letcher B.H., Nislow K.H. 2010. Context-specific influence of water temperature on brook trout growth rates in the field. Freshwater Biology 55: 2253–2264.

Zhong W., Zhang L., Cui Y., Chen. M., Zhu L. 2019. Probing mechanisms for bioaccumulation of perfluoroalkyl acids in carp (Cyprinus carpio): Impacts of protein binding affinities and elimination pathways. Science of The Total Environment 647: 992-999.

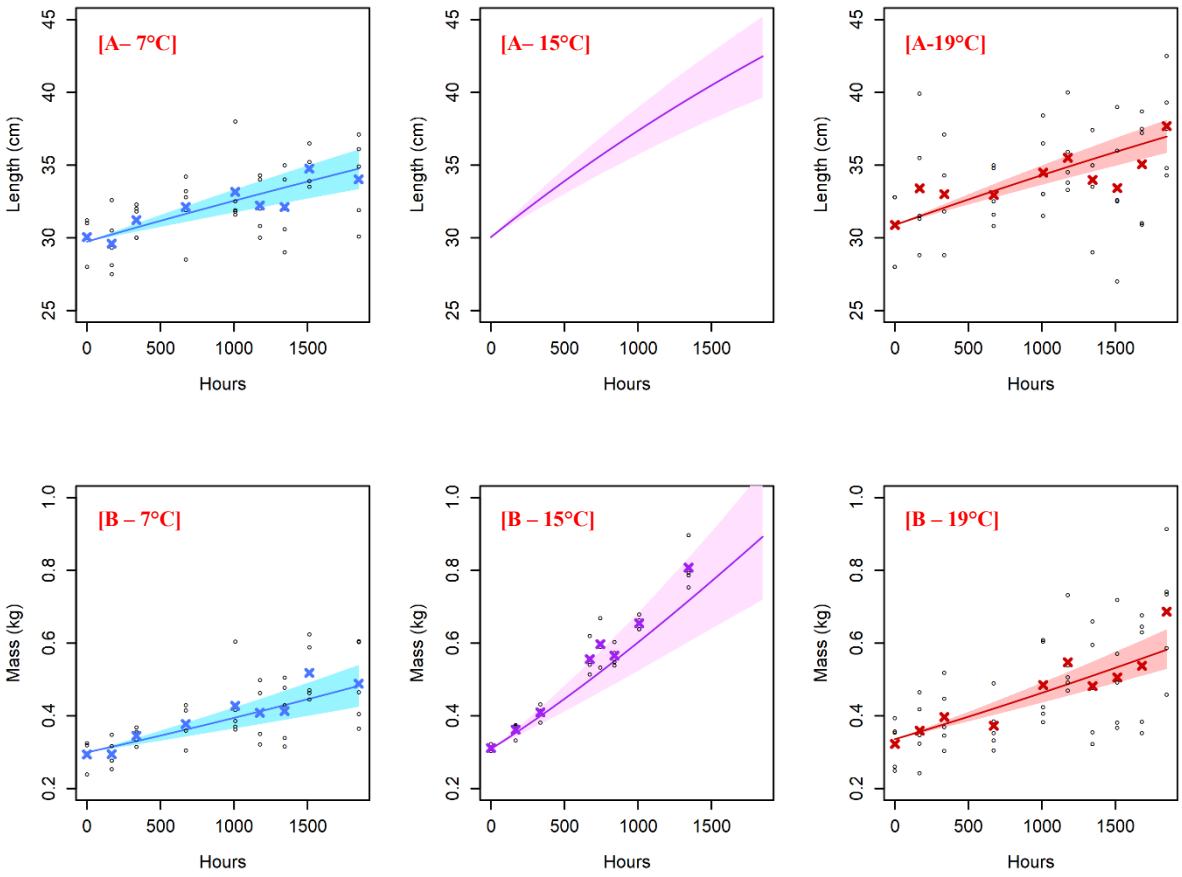

Figure 1. Model predictions of fish length (A) and fish mass (B) at 7°C, 15°C and 19°C (blue, purple and red lines, respectively) and their 95% credibility intervals (coloured areas). Coloured crosses are the arithmetic mean of observed data (n=5) and empty circles are the individual observed data values. The data at 15°C [A–15°C] came from an external dataset (*i.e.* Goeritz et al., 2013) that did not have recorded size data, so only predictions are represented. $\gamma = 0.55$ (IC95% [0.32 – 0.84]), $\gamma = 1.51$ (IC95% [1.08 – 1.97]) and $\gamma = 0.69$ (IC95% [0.44 – 1.01]), for the 7°C, 15°C and 19°C experiments, respectively (Equation 7 and 8). Daily feeding rates were 0.5%, 2.6% and 1.0% of the fish average live weight for 7°C, 15°C and 19 °C experiments, respectively.

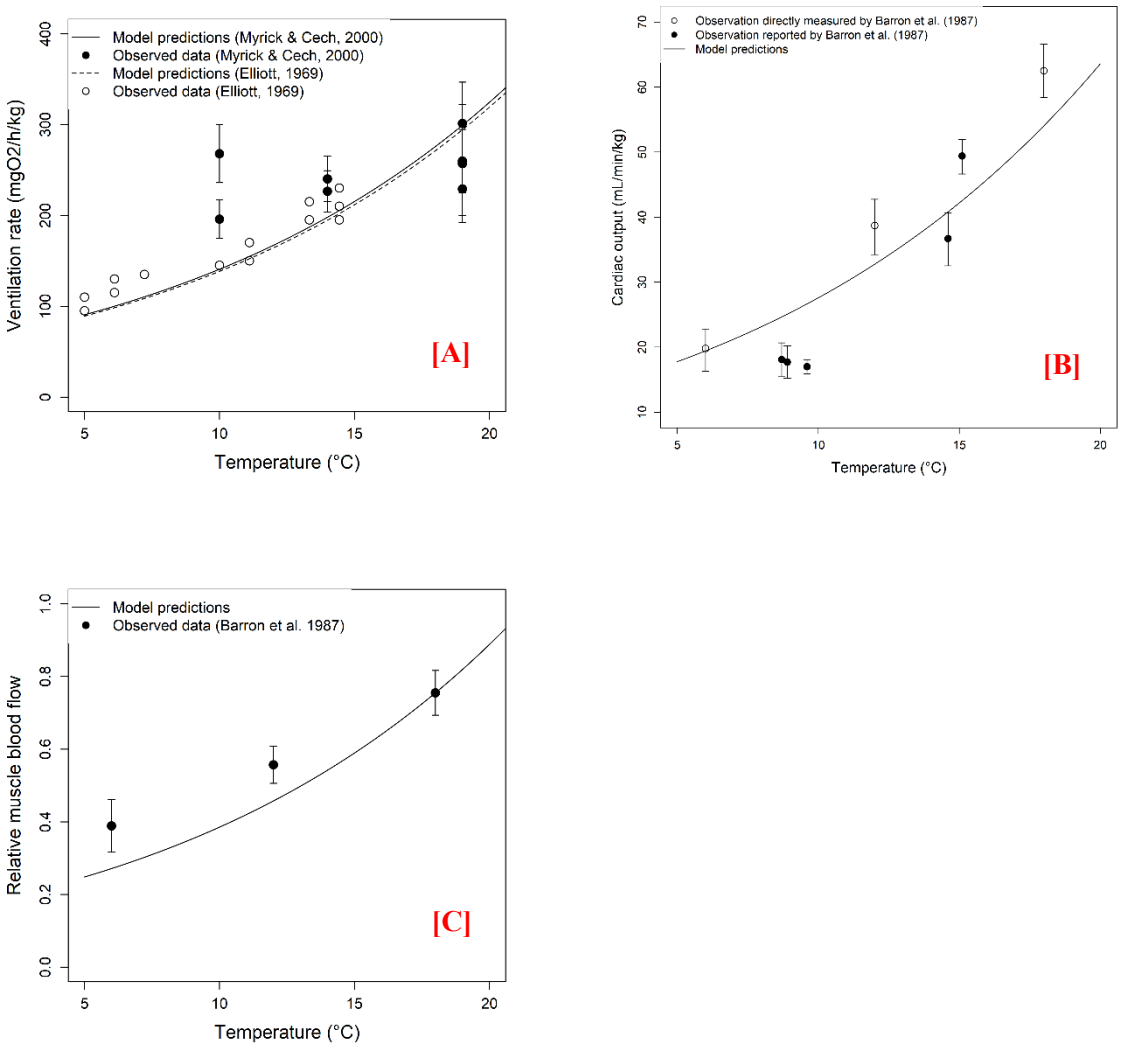

Figure 2. Effects of water temperature on physiological processes. (A) Model predictions of ventilation rate (Equation 3) according to water temperature compared against data recorded by Myrick and Cech (2000) and Elliott (1969). (B) Model predictions of cardiac output (Equation 2) according to water temperature compared against data directly measured by Barron et al. (1987) (predictions were performed using overall mean fish mass of the three groups) or reported by Barron et al. (1987) (Cameron and Davis (1970), Davis and Cameron (1971), Wood and Shelton (1980), Neumann et al. (1983) and Kiceniuk and Jones (1977)). (C) Model predictions of relative blood flow of muscle (Equation 4) against observed data from Barron et al. (1987).

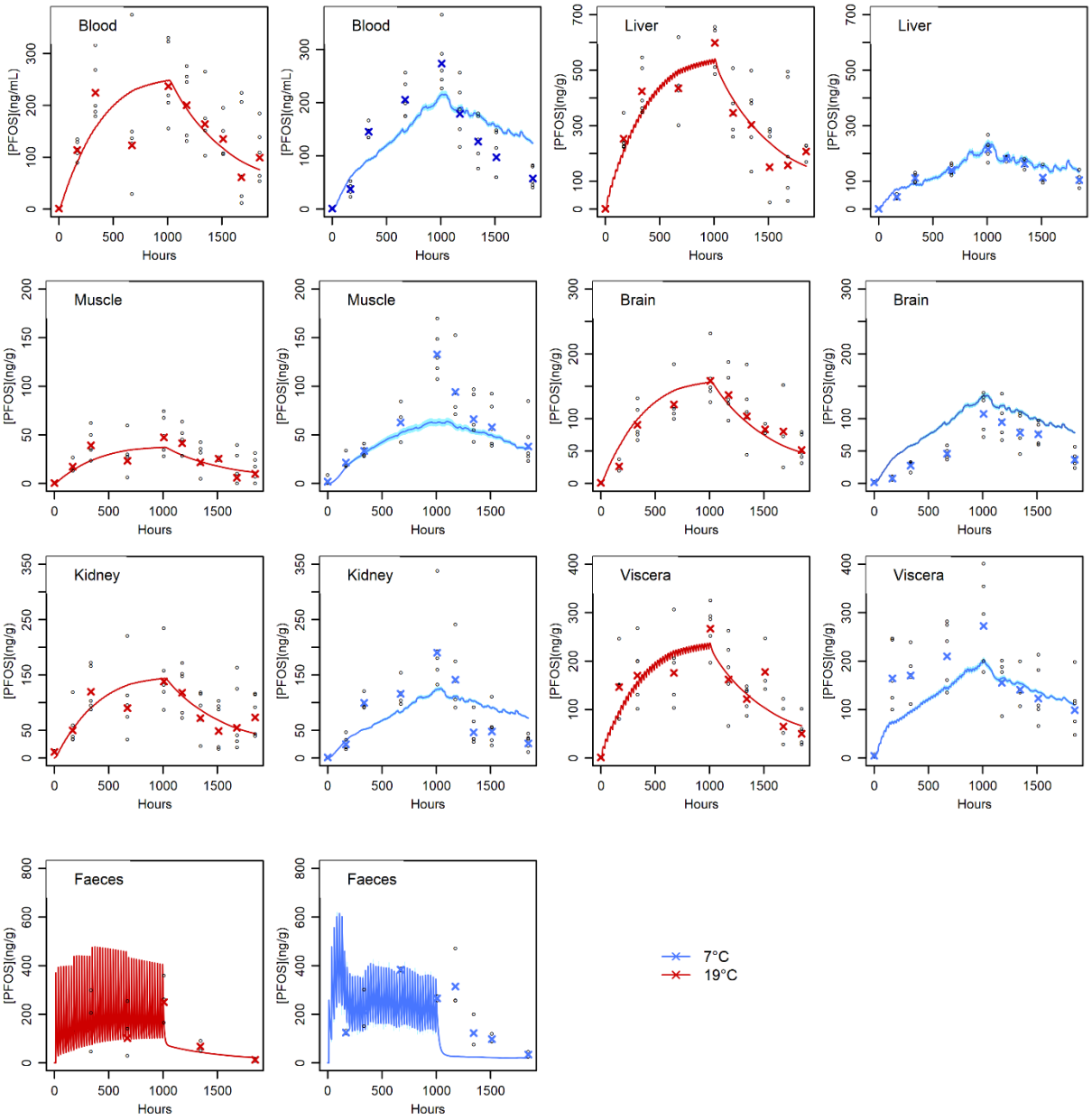

Figure 3. Mean predicted concentrations of PFOS in trout tissues and in faeces at 7°C (blue lines and crosses) and 19°C (red lines and crosses). Lines correspond to model predictions, coloured crosses correspond to observed geometric means (n=5), and empty circles correspond to individual data. Daily oscillations predicted by the model for faeces concentrations (*i.e.* the fraction eliminated by bile and the non-absorbed fraction) were caused by daily feeding intake.

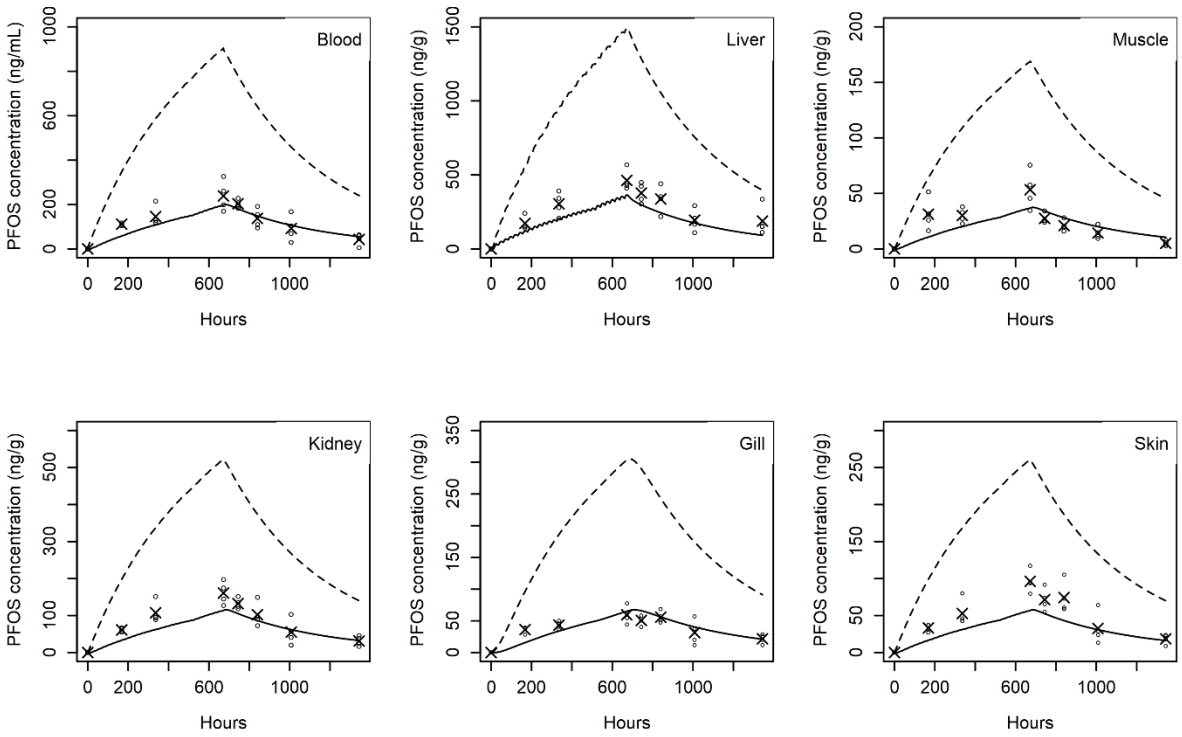

Figure 4. Comparison of predicted PFOS concentrations in fish organs (lines) and measured PFOS concentrations in adult rainbow trout reported by Goeritz et al. 2013 (crosses correspond to observed geometric means and empty circles correspond to individual data). Solid lines correspond to a diet-only exposure (concentration of PFOS in water = 0 ng L^{-1}) and dotted lines correspond to an exposure that was set to the maximum concentration of PFOS in water = 15 ng L^{-1}. Crosses represent means and empty circles correspond to individual data.

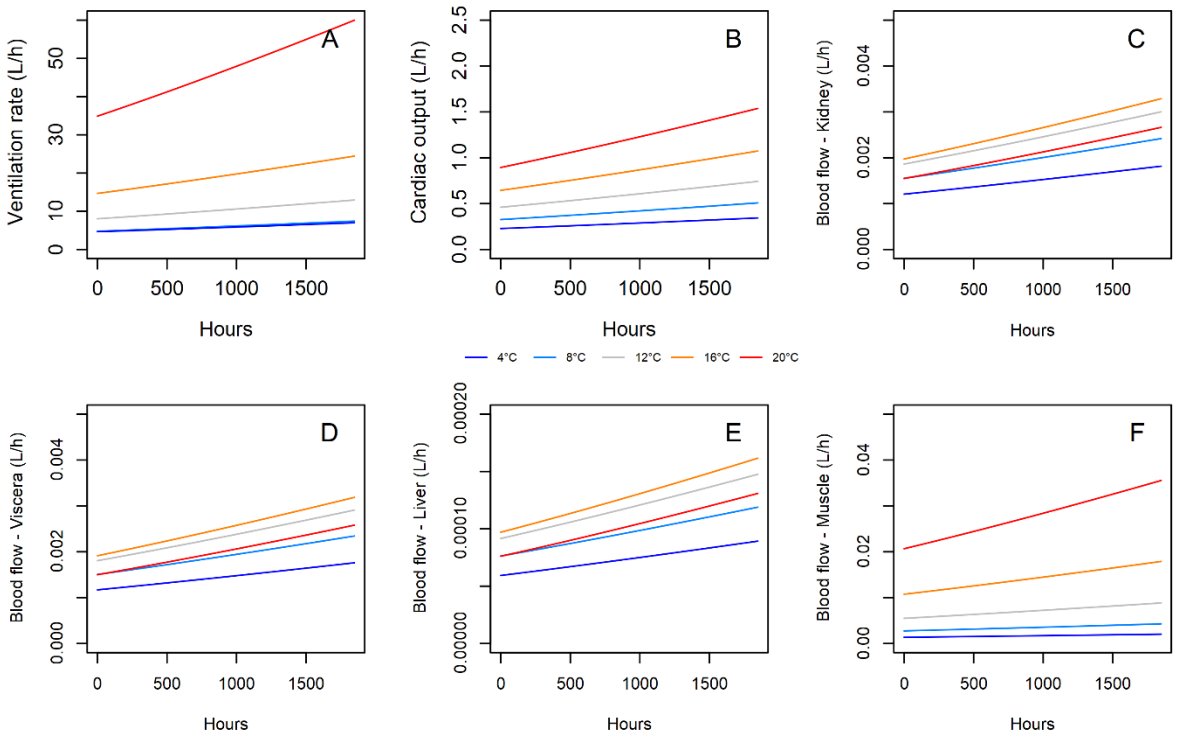

Figure 5. Theoretical effect of temperature on physiological processes: ventilation rate (A), cardiac output (B) and blood flow to the kidney (C), viscera (D), liver (E) and muscle (F). Each colour corresponds to a temperature, *i.e.* 4, 8, 12, 16, 20 °C.

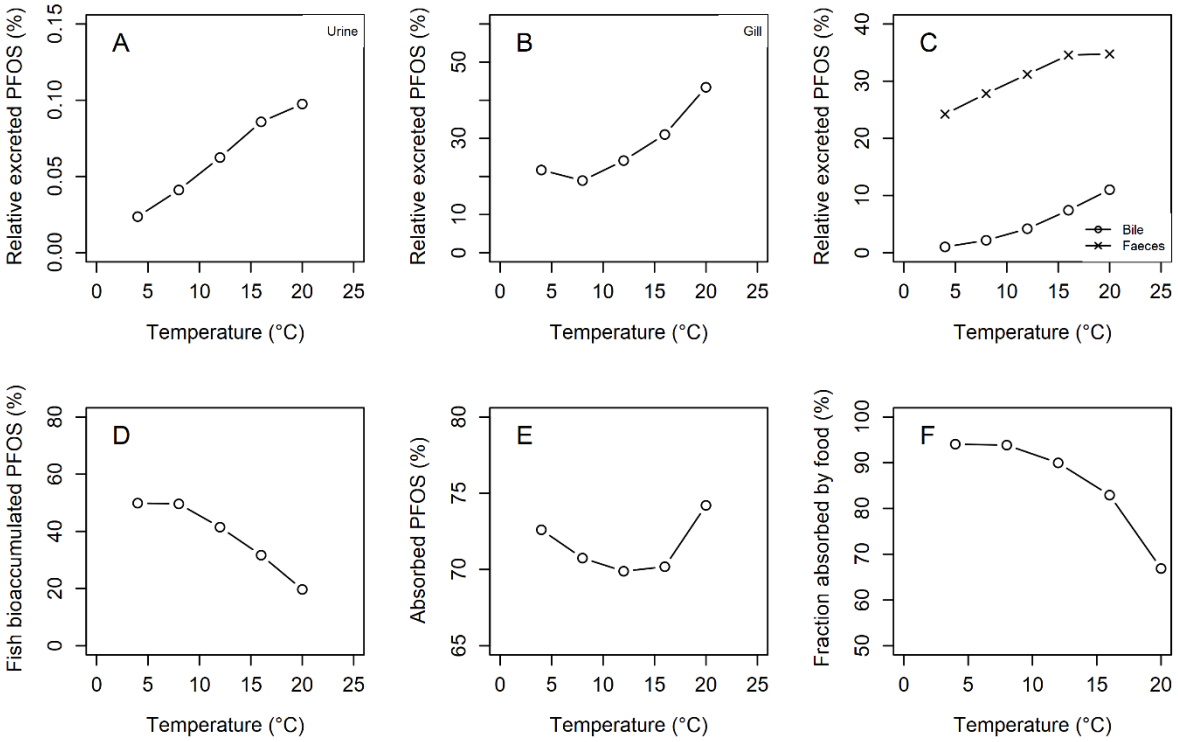

Figure 6. Theoretical effect of temperature on the kinetic processes at 42d (end of the PFOS exposure via diet): urinary excretion (A), gill excretion (B), biliary excretion (C), bioaccumulation in the fish (D), absorption efficiency (E), and fraction of PFOS absorbed by food (F).

Table 1. Symbols, definitions, prior distributions or values, estimations of mean and standard deviation (SD) and 95% CI for all Arrhenius temperatures.

Symbol	Arrhenius temperature of processes	Prior distribution*	Posterior distribution	
			Mean ± SD	95% CI
TA_{Qc}	Cardiac output process	6930 K	6930 K	-
TA_{VO2}	Dynamic dissolved oxygen process	6930 K	6930 K	-
TA_{frac_muscle}	Blood flow to muscle	6930 K	6930 K	-
TA_{PC}	Tissue-blood partition coefficient	N(6930,30%)	5664±251 K	[5180;6149]
TA_{ku}	Absorption process rate	N(6930,30%)	5423±597 K	[4273;6615]
$TA_{clearance}$	Clearance process	N(6930,30%)	8267±779 K	[6799;9822]

*N stands for normal distribution (prior, coefficient variation)

Table 2. BIC values of the different simplified versions of the model.

Sub-model	BIC	BIC ratio
Temperature integrated on all physiological and kinetic processes	2130.5	-
without temperature effects on absorption rate (*ku)*	2291.2	1.08
without temperature effects on *ku* and clearances ($Cl_{bile,}$ $Cl_{faeces,}$ Cl_{urine})	2447.1	1.15
without temperature effects on absorption rate, clearances *and* tissue-plasma partition coefficients (*PC), i.e.* temperature integrated on physiological processes only.	2671.0	1.25

SUPPLEMENTARY INFORMATION

Temperature effect on perfluorooctane sulfonate toxicokinetics in rainbow trout (Oncorhynchus mykiss): exploration via a physiologically based toxicokinetic model

Alice Vidal[a], Marc Babut[a], Jeanne Garric[a], Rémy Beaudouin[b]*

[a] Irstea, UR RIVERLY, 5 Avenue de la Doua, CS20244, 69625 Villeurbanne Cedex, France.

[b] UMR-I 02 SEBIO, Models for Ecotoxicology and Toxicology (METO), INERIS, 60550 Verneuil en Halatte, France.

*Corresponding author: remy.beaudouin@ineris.fr

Summary

6. Section A.1. Ddescription of the model

A.1.1. Schematic description of the PBTK model developed for rainbow trout.

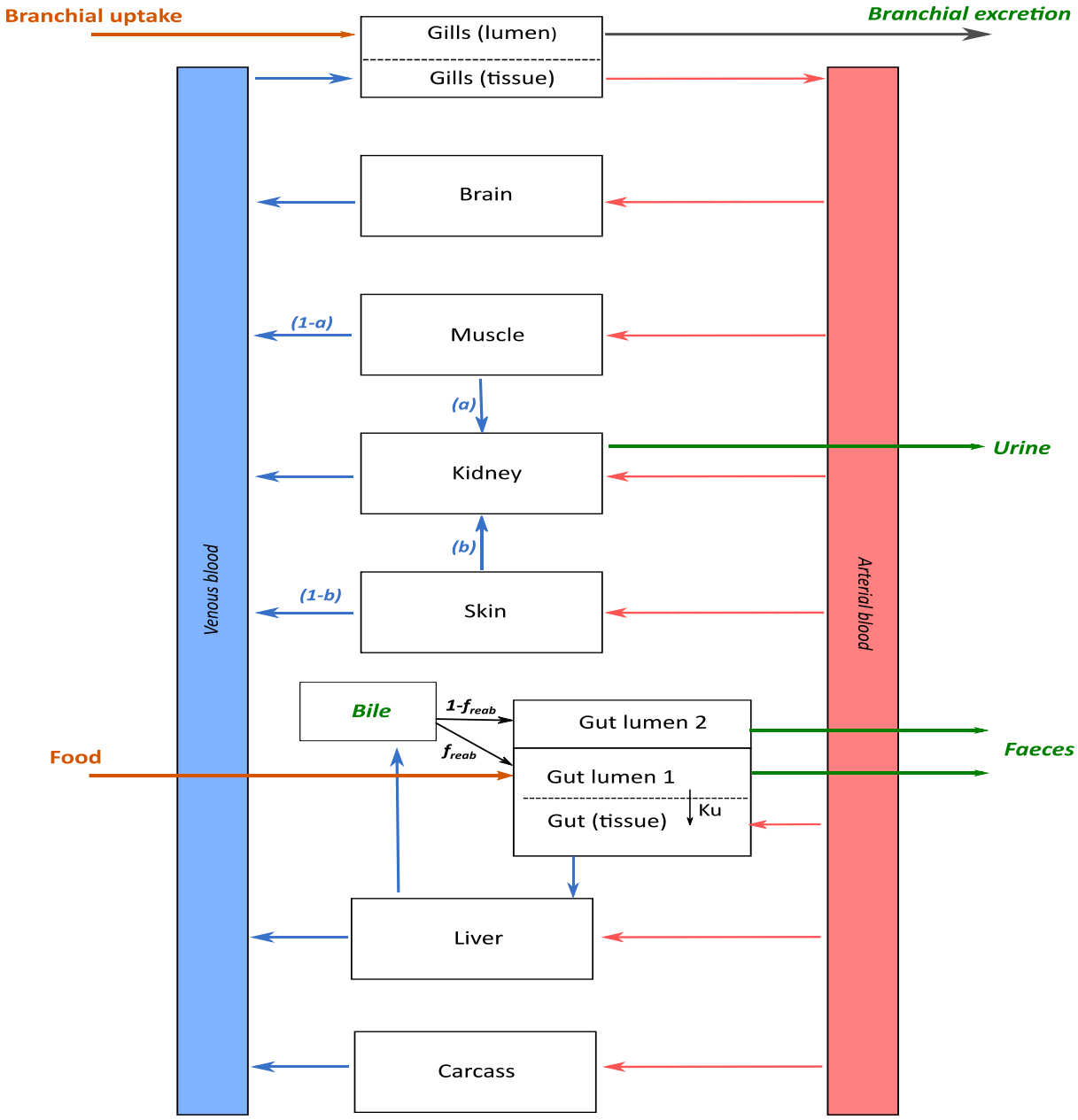

Figure A.1. Schematic description of the PBTK model developed for rainbow trout.

Uptake (food and branchial uptake) and excretion (faeces, urine, bile and branchial excretion) sites are represented in orange and green, respectively. In gut lumen, we distinguished two forms of PFOS. The first was free PFOS, which was absorbed (*gut lumen 1*), and the second was the PFOS conjugated in bile (*gut lumen 2*). In this model, PFOS was not reabsorbed (f_{reab}=0) and the totality of PFOS in bile was assumed to first enter the gut lumen 2, and then get eliminated by faeces. All of the venous blood flowing out of the gut entered the liver and a fraction of venous blood flowing out of muscle and skin

entered the kidney (fractions “a” and “b”, respectively), whereas the remaining flows of both tissues returned to systemic circulation (Nichols *et al.* 1996; Nichols *et al.* 2004). Furthermore, we assumed that there was no PFOS metabolism.

A.1.2. Table A.1. Glossary of parameter symbols, definitions, units and values, and the sources used in the PBTK model.

Symbol	Definition	Units	Value	Sources
Physiological parameters				
VO2ref	Oxygen consumption rate reference	mgO2 h-1 kg -1	135.8	Elliott, 1969
$BWVO2_{ref}$	Reference body weight at which VO2ref was recorded	Kg	1.0	Elliott, 1969
$TVO2_{ref}$	Temperature at which VO2ref was recorded	K	283.7	Elliott, 1969
OEE	Oxygen extraction efficiency	L h-1	0.8	Erickson and McKim (1990)
F_cardref	Cardiac output reference	L h-1 kg -1	1.19	Baron *et al.* 1987
TF_{card_ref}	Temperature at which F_cardref was recorded	K	279.2	Baron *et al.* 1987
BWF_{card_ref}	Reference body weight at which F_cardref was recorded	Kg	0.27	Baron *et al.* 1987
TA		K	6930	Grech *et al.* 2017
Texp		K	191.8	Vidal et al. 2019
Frac_*i*	Relative fraction of arterial blood to tissue *i*	-		
Liver			0.004	Baron *et al.* 1987
Muscle			0.655	Baron *et al.* 1987
Kidney			0.071	Baron *et al.* 1987
Viscera			0.069	Baron *et al.* 1987
Brain			0.055	Péry *et al.* 2014
Skin			0.073	Nichols *et al.* 1996
Gill			0.0002	Baron *et al.* 1987
Sc_*i***	Fraction of body weight	-		
Blood			0.045	Gingerich *et al.* 1990
Liver			0.012	This study
Muscle			0.566	This study
Kidney			0.016	This study
Viscera			0.051	This study
Brain			0.001	This study
Skin			0.064	Goeritz *et al.* 2013
Gill			0.020	Goeritz *et al.* 2013
Lumen			0.001	Nichols *et al.* 1996
a	Fraction of muscle going to kidney		0.6	Nichols *et al.* 1990
b	Fraction of skin going to kidney		0.9	Nichols *et al.* 1990
Plasma	Fraction of plasma in trout	%	0.7	Stevens, 1968; Brill et al. 1998; Barron et al. 1987;Gingerich and Pityer, 1989
Free	Free PFOS in plasma	%	$3.2\ 10\text{-}2 \pm 0.6\ 10^{-2}$	Vidal *et al.* 2019b

freab	Reabsorbed PFOS fraction	-	0.0	Vidal *et al.* 2019b
Biometric parameters				
Lm	Maximum length	cm	73.91±14.85	Fishbase*
γ	Effect of food availability and temperature on growth rate	-	7°C : 0.55 ± 0.13 19°C : 0.69 ± 0.15	This study
κ	Growth rate	cm h-1	0.0096 ± 0.0020	-
α	Constants in the allometric growth equation	-	1.08 10-5±3.94 10^{-6}	Grech *et al.* 2017
β		-	3.03±0.10	Grech *et al.* 2017
Substance-specific parameters				
PC_*i*	Tissue *i* blood partition coefficient			
Liver		-	2.05±0.13	Vidal *et al.* 2019b
Muscle		-	0.15±0.01	Vidal *et al.* 2019b
Kidney		-	0.58±0.04	Vidal *et al.* 2019b
Viscera		-	0.87±0.09	Vidal *et al.* 2019b
Brain		-	0.63±0.04	Vidal *et al.* 2019b
Skin		-	0.25	Goeritz *et al.* 2013
Gills		-	0.40	Goeritz *et al.* 2013
$PCblood_{:water}$	Blood-water partition coefficient	-		Vidal *et al.* 2019b
Clurine	Urinary clearance	L h-1	0.07±0.01	Consoer *et al.* 2016
Clbile	Biliary clearance	L h-1	2.16 10-3±0.37 10^{-3}	Vidal *et al.* 2019b
Clfaeces	Faecal clearance	L h-1	2.62 10-4±0.14 10^{-4}	Vidal *et al.* 2019b
Ku	Absorption rate constant	h-1	0.13±0.013	Vidal *et al.* 2019b

*http://fishbase.org/search.php

A.1.3. Model equations

PFOS absorption

In gut lumen, we distinguished two forms of PFOS. the first was free PFOS, which was absorbed (*gut lumen 1*), and the second was the PFOS conjugated in bile (*gut lumen 2*).

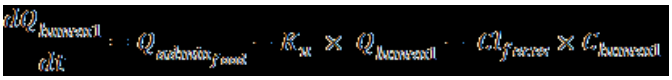

(Equation A.1)

where Q_{lumen1} is the amount of PFOS that transfers into gut lumen 1, $Qadmin_{food}$ is the amount of PFOS ingested by food (ng), Ku is the absorption rate constant (h^{-1}), Cl_{faeces} is faecal clearance ($L\ h^{-1}$) and C_{lumen1} is the PFOS concentration in gut lumen 1 compartment ($ng\ g^{-1}$).

$$\frac{dQ_{lumen2}}{dt} = \frac{dQexcret\_bile}{dt} - Cl_{faeces} \times C_{lumen2} \qquad \textbf{(Equation A.2)}$$

where Q_{lumen2} is the amount of PFOS that transfers into gut lumen 2, and C_{lumen2} is the PFOS concentration in the gut lumen 2 compartment ($ng\ g^{-1}$).

$$\frac{dQadmin_{gill}}{dt} = Q_w \times C_{water} \qquad \textbf{(Equation A.3)}$$

where $Qadmin_{gill}$ is the quantity of PFOS absorbed into blood (ng) and C_{water} corresponds to PFOS concentrations in water ($ng\ L^{-1}$).

$$Q_w = \frac{VO_2}{OEE * C_{ox}}\ \textbf{, L.h}^{-1} \qquad \textbf{(Equation A.4)}$$

where Cox is dissolved oxygen concentration in water ($mgO_2\ L^{-1}$), VO_2 is oxygen consumption rate ($mgO_2\ h^{-1}$) and OEE is oxygen extraction efficiency set to 0.8, as proposed by Erickson and McKim (1990).

Dissolved oxygen concentrations in water were measured during the experiments, and the experimental values were used for the different simulations. This data is reported in SI Table A.3.

PFOS distribution through the organism

We assume that all tissue compartments are homogeneous and distribution is limited by flow. Flows to tissues were calculated considering the free fraction of PFOS in plasma.

$$\frac{d(Q_i)}{dt} = F_i \times Free \times \left(Cart(t) - \frac{C_i(t)}{PC_i}\right) \qquad \textbf{(Equation A.5)}$$

where Qi is amount of chemical in compartment i, Fi is the arterial plasma blood flow to compartment i, $Free$ is free fraction of PFOS, $Cart$ is chemical concentration in arterial blood, Ci is chemical concentration in venous blood leaving compartment i, and t is time. Fi was calculated by multiplying the relative fraction of each organ ($Frac_i$) by the cardiac output and volume of each organ, making it possible to calculate Ci, which was obtained by multiplying the organ fraction (Sc_i) by body weight. PC_i is the tissue i plasma partition coefficient.

PFOS elimination

Dynamic equations for PFOS elimination by bile, faeces and urine were dependent on PFOS concentrations in the liver, gut lumen and kidney, respectively.

$$\frac{dQexcret_{bile}}{dt} = Cl_{bile} \times Free \times C_{liver} \quad \textbf{(Equation A.6)}$$

where $Qexcret_{bile}$ is the amount of PFOS excreted into the bile (ng), Cl_{bile} is biliary clearance (L h^{-1}) and C_{liver} is PFOS concentration in liver (ng g^{-1}).

In this model, the totality of PFOS in bile was assumed to enter the gut lumen 2, and then get eliminated via faeces. This route represents the fraction of PFOS eliminated by bile and the fraction unabsorbed.

$$\frac{dQexcret_{faeces}}{dt} = Cl_{faeces} \times (C_{lumen1} + C_{lumen2}) \quad \textbf{(Equation A.7)}$$

where $Qexcret_{faeces}$ corresponds to the amount of PFOS eliminated in the faeces (ng).

$$\frac{dQexcret_{urine}}{dt} = Cl_{urine} \times Free \times \frac{C_{kidney}}{PC_{kidney}} \quad \textbf{(Equation A.8)}$$

where $Qexcret_{urine}$ is the amount of PFOS excreted into urine (ng), Cl_{urine} is urinary clearance (L h^{-1}), C_{kidney} is PFOS concentration in the kidney (ng g^{-1}) and PC_{kidney} is the plasma-kidney partition coefficient. In this submodel, we did not consider potential PFOS reabsorption by urine.

$$\frac{dQexcret_{gill}}{dt} = Q_w \times Free \times \frac{C_{venous}}{\mathrm{PC_{blood:water}}} \quad \textbf{(Equation A.9)}$$

where $Qexcret_{gill}$ is the amount of PFOS eliminated by gills (ng), C_{venous} is the PFOS concentration in venous blood (ng L^{-1}) and $PC_{blood:water}$ is the blood-water partition coefficient.

7. Section A.2. Model inputs

A.2.1. PFOS concentrations in food

Measured PFOS concentrations in the spiked food batch used for the experiments at 7°C and 19°C were 465.1±26.0 ng g^{-1} dw and 452.8±27.1 ng g^{-1} dw, respectively.

A.2.2. Table A.2. PFOS concentrations in water

	PFOS concentrations (ng L^{-1})	
Days	**Tanks at 7°C**	**Tanks at 19°C**
7	1.19	1.01
14	1.00	0.81
28	1.45	0.74
42	1.15	0.65
49	2.29	0.52
56	1.51	0.41
63	0.60	-
70	-	0.43
77	3.31	2.15

A.2.3. Table A.3. Oxygen concentration

	Oxygen concentration (mg O2/ L)	
	Tanks at 7°C	**Tanks at 19°C**
	11.44 ± 1.02	8.05 ± 0.33

A.2.4. Water temperatures

For the experiment conducted at 19°C, temperature variations were negligible. Therefore, the water temperature indicated in the model is the mean of the daily measured values (18.26 ± 0.73°C).

For the experiment conducted at 7°C, it was more difficult to maintain a constant water temperature due to rapid variations during the experimental period (between January and March 2017). Daily records for this experiment are reported in Figure A.2, below. Therefore, the water temperatures integrated into the model were daily mean temperatures.

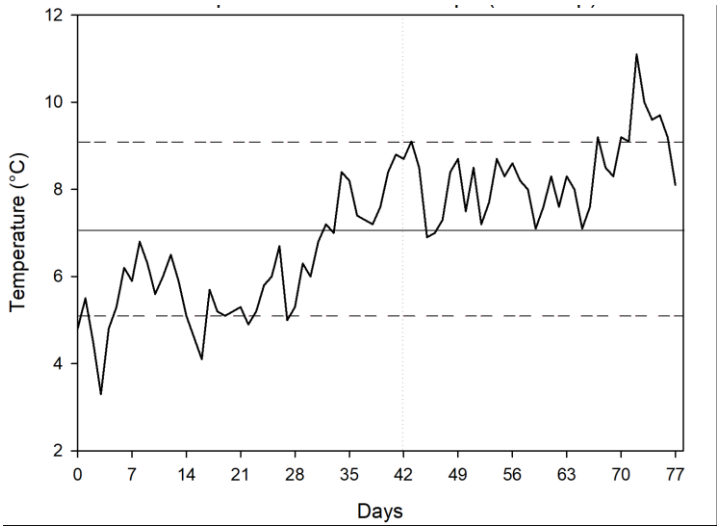

Figure A.2. Daily water temperature records during the experiment conducted at 7°C (Vidal et al. 2019a).

Table A.4 Daily mean temperatures for the experiment conducted at 7°C (inputs to the model)

Date	Mean temperature (°C)	Date	Mean temperature (°C)	Date	Mean temperature (°C)
04/01/2017	4.8	31/01/2017	5	27/02/2017	8.7
05/01/2017	5.5	01/02/2017	5.3	28/02/2017	8.3
06/01/2017	4.5	02/02/2017	6.3	01/03/2017	8.6
07/01/2017	3.3	03/02/2017	6	02/03/2017	8.2
08/01/2017	4.8	04/02/2017	6.8	03/03/2017	8
09/01/2017	5.3	05/02/2017	7.2	04/03/2017	7.1
10/01/2017	6.2	06/02/2017	7	05/03/2017	7.6
11/01/2017	5.9	07/02/2017	8.4	06/03/2017	8.3
12/01/2017	6.8	08/02/2017	8.2	07/03/2017	7.6
13/01/2017	6.3	09/02/2017	7.4	08/03/2017	8.3
14/01/2017	5.6	10/02/2017	7.3	09/03/2017	8
15/01/2017	6	11/02/2017	7.2	10/03/2017	7.1
16/01/2017	6.5	12/02/2017	7.6	11/03/2017	7.6
17/01/2017	5.9	13/02/2017	8.4	12/03/2017	9.2
18/01/2017	5.1	14/02/2017	8.8	13/03/2017	8.5
19/01/2017	4.6	15/02/2017	8.7	14/03/2017	8.3
20/01/2017	4.1	16/02/2017	9.1	15/03/2017	9.2
21/01/2017	5.7	17/02/2017	8.5	16/03/2017	9.1
22/01/2017	5.2	18/02/2017	6.9	17/03/2017	11.1
23/01/2017	5.1	19/02/2017	7	18/03/2017	10
24/01/2017	5.2	20/02/2017	7.3	19/03/2017	9.6
25/01/2017	5.3	21/02/2017	8.4	20/03/2017	9.7
26/01/2017	4.9	22/02/2017	8.7	21/03/2017	9.2
27/01/2017	5.2	23/02/2017	7.5	22/03/2017	8.1
28/01/2017	5.8	24/02/2017	8.5		

29/01/2017	6	25/02/2017	7.2
30/01/2017	6.7	26/02/2017	7.7

A.2.5. Initial fish length and weight

T(°C)	Length (cm)	Weight (kg)
7	30.1 ± 1.5	0.294 ± 0.039
19	30.9 ± 2.6	0.323 ± 0.064

8. Section A.3. Additional results.

A.3.1. Predictions of the model without the temperature effects

We applied the 7°C experiment exposure scenario to the model calibrated on the 19°C experimental data. Results of the predictions showed that direct application of the exposure scenario did not perform well enough to correctly explain fish growth or PFOS concentrations in tissues. This confirms that water temperature is a key variable to consider for describing PFOS TK.

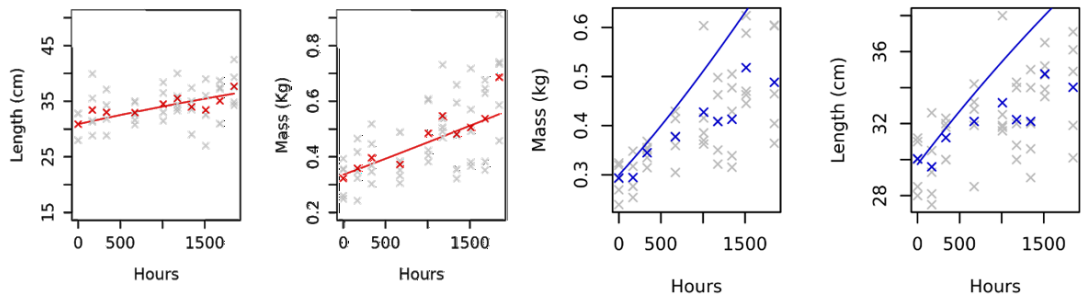

Figure A.3. Predictions of fish growth at 7°C and 19°C based on direct application of the PBTK model calibrated on data observed at 19°C. Processes were not temperature-corrected. Lines correspond to the model predictions, coloured crosses correspond to observed means, and grey crosses correspond to individual data. Red lines and crosses correspond to the 19°C experiment, and blue lines and crosses correspond to the 7°C experiment.

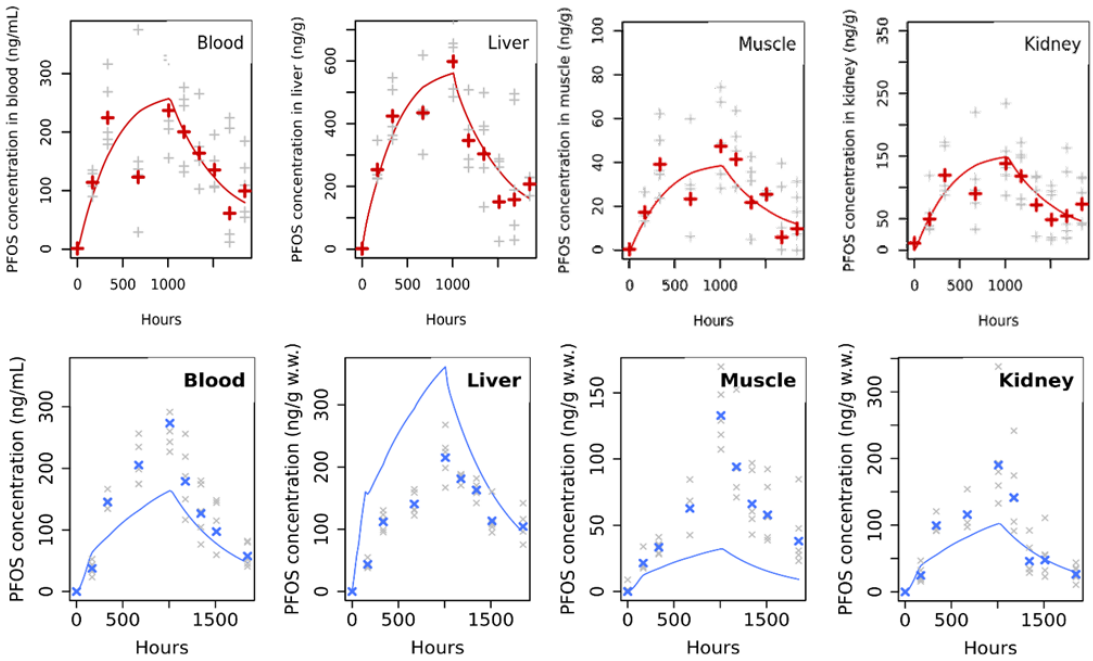

Figure A.4. Predicted PFOS concentrations in target tissues at 7°C and 19°C without any temperature correction of the processes. Lines correspond to the model predictions, coloured crosses correspond to observed means, and grey crosses correspond to individual data. Red lines and crosses correspond to the 19°C experiment, and blue lines and crosses correspond to the 7°C experiment.

A.3.2. Chain convergence diagnostic

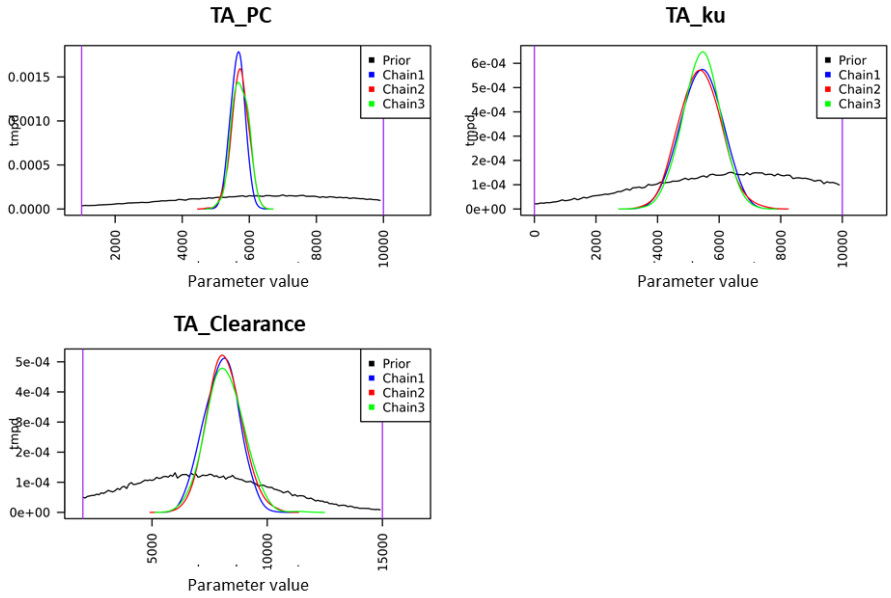

Figure A.5a. Chain convergence diagnostic. For all parameters, density of the prior is represented by the black line and density of the posterior by the coloured line, with chain 1, chain 2 and chain 3 in blue, red and green, respectively.

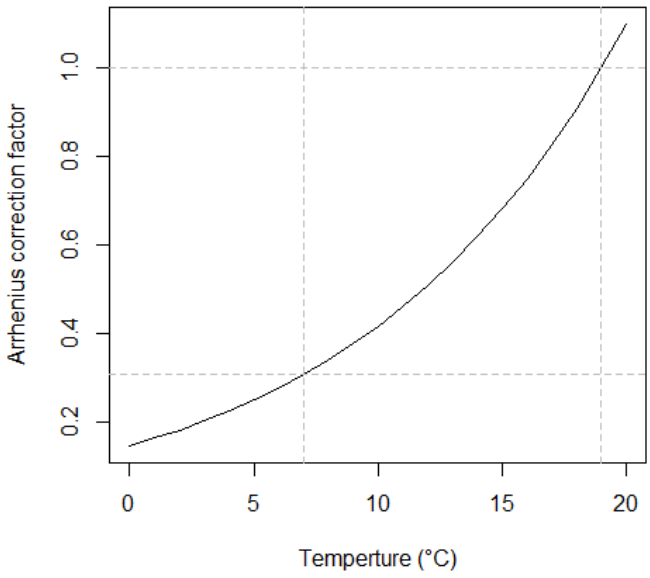

Figure A.5b. Arrhenius correction factor for the urine, faeces and bile elimination rate (TA_clearance). Grey lines represent the values of the correction factor at 7°C and 19°C.

A.3.3. Observations vs. predictions.

Coloured crosses represent mean PFOS concentrations in organs. The red line represents a 1-fold factor, and dotted lines represent 1.5-fold and 2-fold factors.

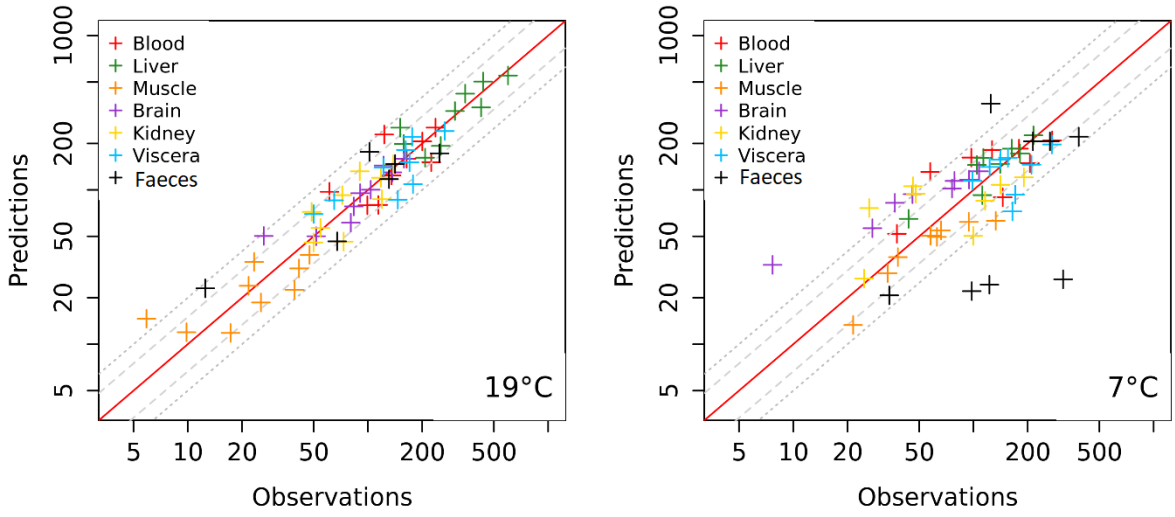

Figure A.6. Comparison between observed and predicted data after model calibration. Coloured crosses represent mean PFOS concentrations in target organs. The red line represents a 1-fold factor, and dotted lines represent 1.5-fold and 2-fold factors.

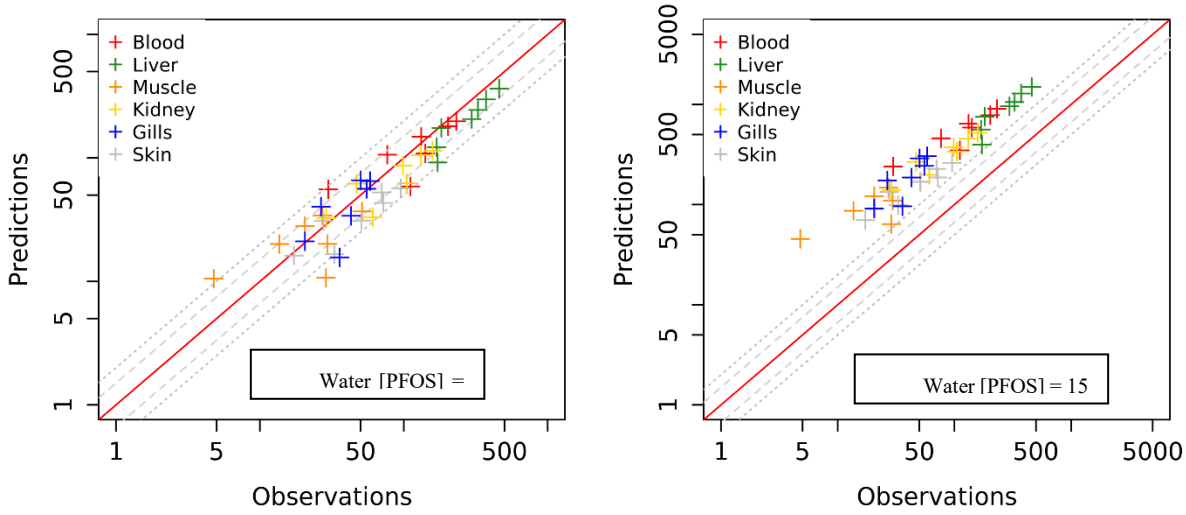

Figure A.7. Comparison between observed and predicted data (Goeritz et al., 2013). The left panel represents the scenario without water exposure, and the right panel plots predictions using the worst-case scenario (constant exposure to the maximum value reported). Coloured crosses represent mean PFOS concentrations in target organs. The red line represents a 1-fold factor, and dotted lines represent 1.5-fold and 2-fold factors.

References

Barron, M.G., Tarr, B.D., Hayton, W.L., 1987. Temperature-dependence of cardiac output and regional blood flow in rainbow trout, Salmo gairdneri Richardson. J. Fish Biol. 31, 735–744. doi:10.1111/j.1095-8649.1987.tb05276.x

Brill, R.W., Cousins, K.L., Jones, D.R., Bushnell, P.G., & Steffensen, J.F. 1998. Blood volume, plasma volume and circulation time in a high-energy-demand teleost, the yellowfin tuna (*Thunnus albacares*), J. Exp. Biol. 654, 647–654.

Consoer, D.M., Hoffman, A.D., Fitzsimmons, P.N., Kosian, P.A., Nichols, J.W., 2016. Toxicokinetics of Perfluorooctane Sulfonate in Rainbow Trout (Oncorhynchus Mykiss). Environ. Toxicol. Chem. 35, 717–727. doi:10.1002/etc.3230

Elliott, J. W., 1969. The Oxygen Requirements of Chinook Salmon. The Progressive Fish-Culturist. 31, 67-73.

Erickson, R. J., McKim, J. M., 1990. A model for exchange of organic chemicals at fish gills: flow and diffusion limitations. Aquat. Toxicol. 18, 175-197.

Gingerich, W.H., Pityer, R.A., Rach, J.J. 1990. Whole body and tissue blood volumes of two strains of rainbow trout (Oncorhynchus mykiss). Comp. Biochem. Physiol. 97, 615–620.

Goeritz, I., Falk, S., Stahl, T., Schäfers, C., Schlechtriem, C., 2013. Biomagnification and tissue distribution of perfluoroalkyl substances (PFASs) in market-size rainbow trout (Oncorhynchus mykiss). Environ. Toxicol. Chem. 32, 2078–2088. doi:10.1002/etc.2279

Grech, A., Brochot, C., Dorne, J.-L., Quignot, N., Bois, F. Y., Beaudouin, R. 2017. Toxicokinetic models and related tools in environmental risk assessment of chemicals. Sci. Total Environ., 578, 1–15. doi:10.1016/j.scitotenv.2016.10.146

Nichols, J. W., Fitzsimmons, P. N., Whiteman, F. W., Dawson, T. D., Babeu, L., Juenemann, J., 2004. A physiologically based toxicokinetic model for dietary uptake of hydrophobic organic compounds by fish: I. Feeding studies with 2,2',5,5'-tetrachlorobiphenyl. Toxicol. Sci. 77, 206-18.

Nichols, J. W., McKim, J. M., Andersen, M. E., Gargas, M. L., Clewell, H. J., Erickson, R. J., 1990. A physiologically based toxicokinetic model for the uptake and disposition of waterborne organic chemicals in fish. Toxicology and Applied Pharmacology. 106, 433-447.

Nichols, J. W., McKim, J. M., Lien, G. J., Hoffman, A. D., Bertelsen, S. L., Elonen, C. M., 1996. A physiologically based toxicokinetic model for dermal absorption of organic chemicals by fish. Fundam. Appl. Toxicol. 31, 229-242.

Stevens, E.D. 1968. The effect of exercise on the distribution of blood to various organs in rainbow trout. Comp. Biochem. Physiol. 25, 615–625.

Vidal, A., Lafay, F., Daniele, G., Vulliet, E., Rochard, E., Garric, J., & Babut, M. 2019. Does water temperature influence the distribution and elimination of perfluorinated substances in rainbow trout (Oncorhynchus mykiss). Env. Sci. Pollut. Res. 26, 16355 – 16365. https://doi.org/10.1007/s11356-019-05029-w

Vidal, A., Babut, M., Garric, J., & Beaudouin, R. 2019b. Elucidating the fate of perfl uorooctanoate sulfonate using a rainbow trout (Oncorhynchus mykiss) physiologically-based toxicokinetic model. Sci. Total Environ. 691, 1297–1309. https://doi.org/10.1016/j.scitotenv.2019.07.105